A Micromechanics Finite Element Model for Studying the Mechanical Behavior of Spray-On Foam Insulation (SOFI)

Louis J. Ghosn
Ohio Aerospace Institute
Brook Park, Ohio

Roy M. Sullivan and Bradley A. Lerch
NASA Glenn Research Center
Cleveland, Ohio

Proposed Abstract for the
43rd Annual Technical Meeting
Society of Engineering Science
August 13-16th, 2006

A micromechanics model has been constructed to study the mechanical behavior of spray-on foam insulation (SOFI) for the external tank. The model was constructed using finite elements representing the fundamental repeating unit of the SOFI microstructure. The details of the micromechanics model were based on cell observations and measured average cell dimensions discerned from photomicrographs. The unit cell model is an elongated Kelvin model (fourteen-sided polyhedron with 8 hexagonal and six quadrilateral faces), which will pack to a 100% density. The cell faces and cell edges are modeled using three-dimensional 20-node brick elements. Only one-eighth of the cell is modeled due to symmetry.

By exercising the model and correlating the results with the macro-mechanical foam behavior obtained through material characterization testing, the intrinsic stiffness and Poisson's Ratio of the polymeric cell walls and edges are determined as a function of temperature. The model is then exercised to study the unique and complex temperature-dependent mechanical behavior as well as the fracture initiation and propagation at the microscopic unit cell level.

A Micromechanics Finite Element Model for Studying the Mechanical Behavior of Spray-On Foam Insulation

Louis J. Ghosn
Senior Researcher
Ohio Aerospace Institute

Roy M. Sullivan
Material Research Engineer
NASA Glenn Research Center

Bradley A. Lerch
Principal Scientist
NASA Glenn Research Center

43rd Annual Technical Meeting
Society of Engineering Science
August 13-16th, 2006

Micrographs of the Three Major NASA's SOFI Materials

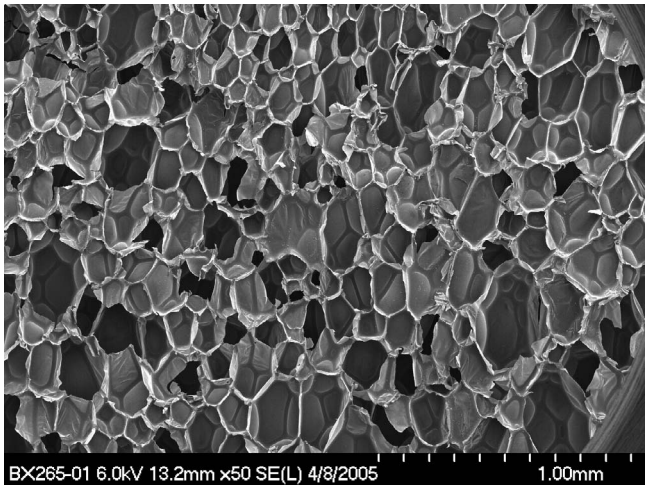

BX-265

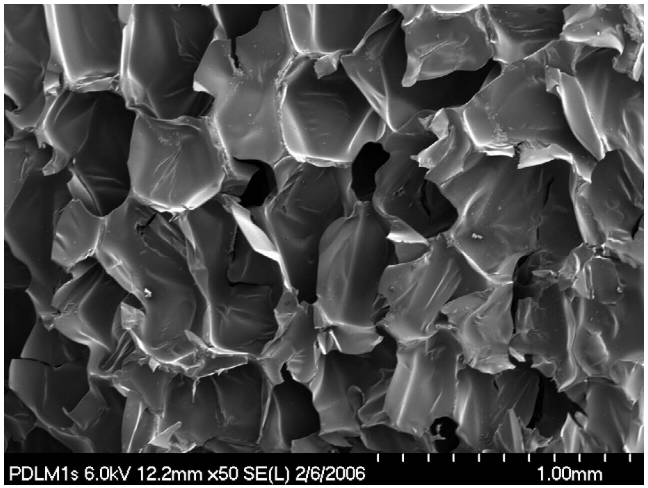

PDL

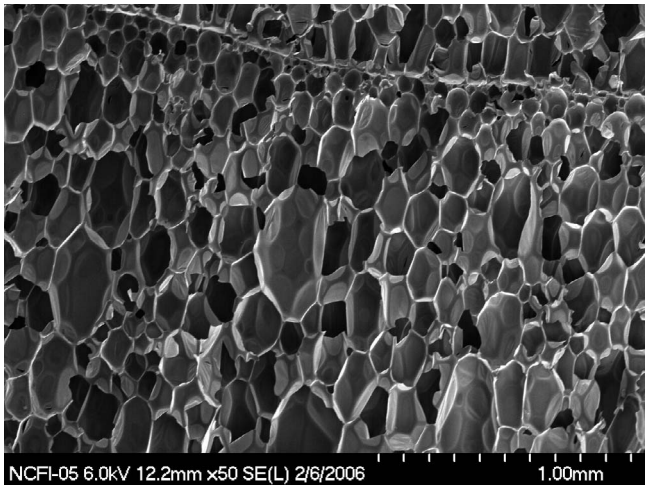

NCFI

Classical Three-Dimensional Polyhedral Cells

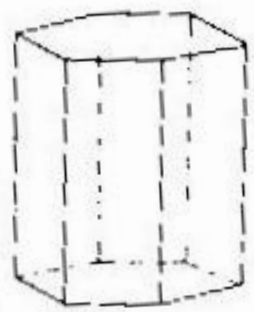

Hexagonal Prism
8 faces, 18 edges
Packs to fill volume ✓

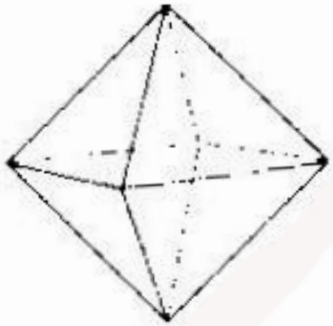

Octahedron
8 faces, 12 edges

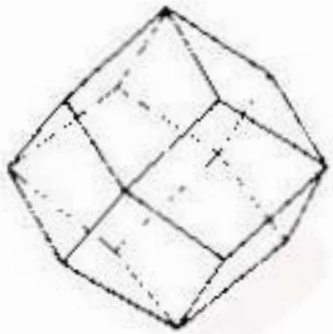

Rhombic dodecahedron
12 faces, 24 edges
Packs to fill volume ✓

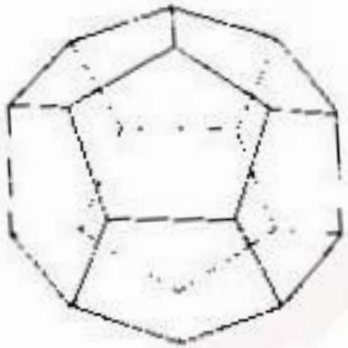

Pentagonal Dodecahedron
12 faces, 30 edges

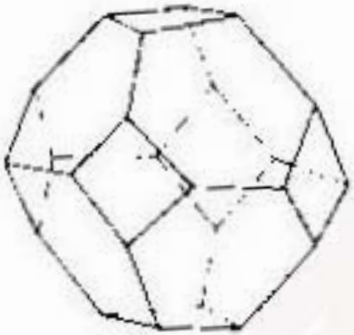

Tetrakaidecahedron
14 faces, 36 edges
Packs to fill volume ✓

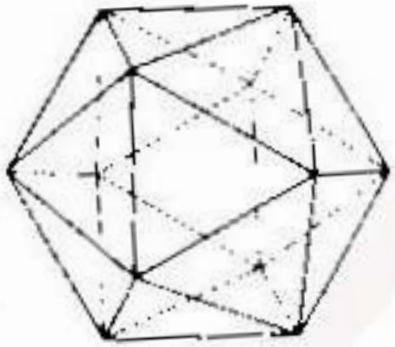

Icosahedron
20 faces, 30 edges

BX-265

Rise Direction

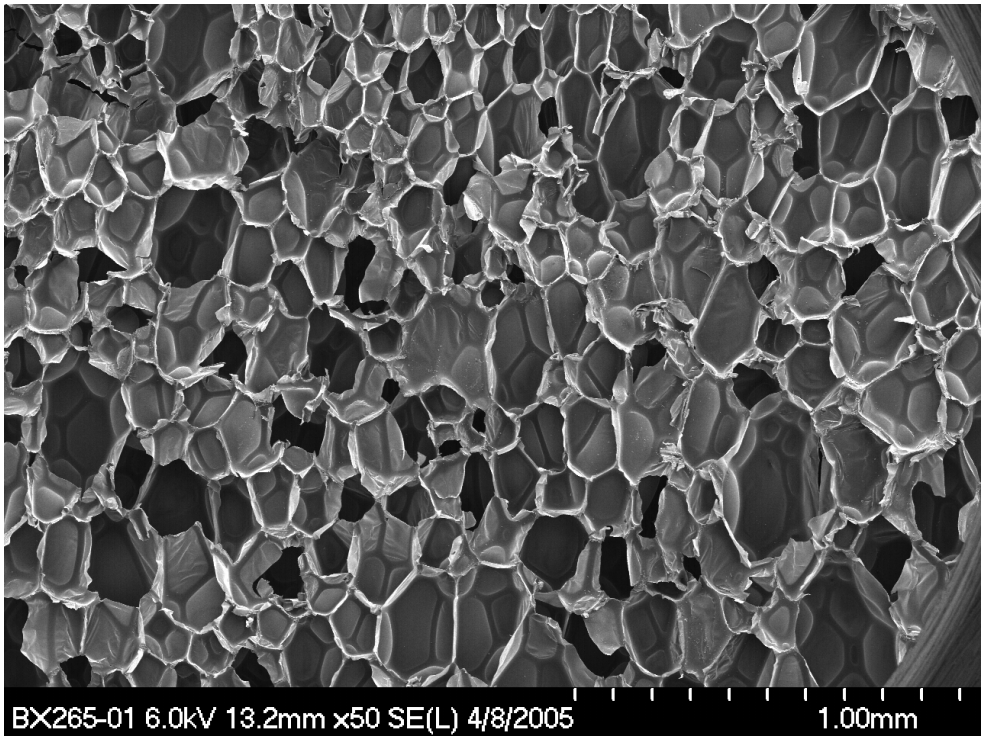

- Average Cell Length (parallel to rise) – 218 μm
- Average Cell Width (perpendicular to rise) – 124 μm
    - Average measured # of faces = 12.4
    - Observed elongated cell structure
- Cells consist of thick edges and thin faces

Assumed Elongated Tetrakaidechahedron

BX-265

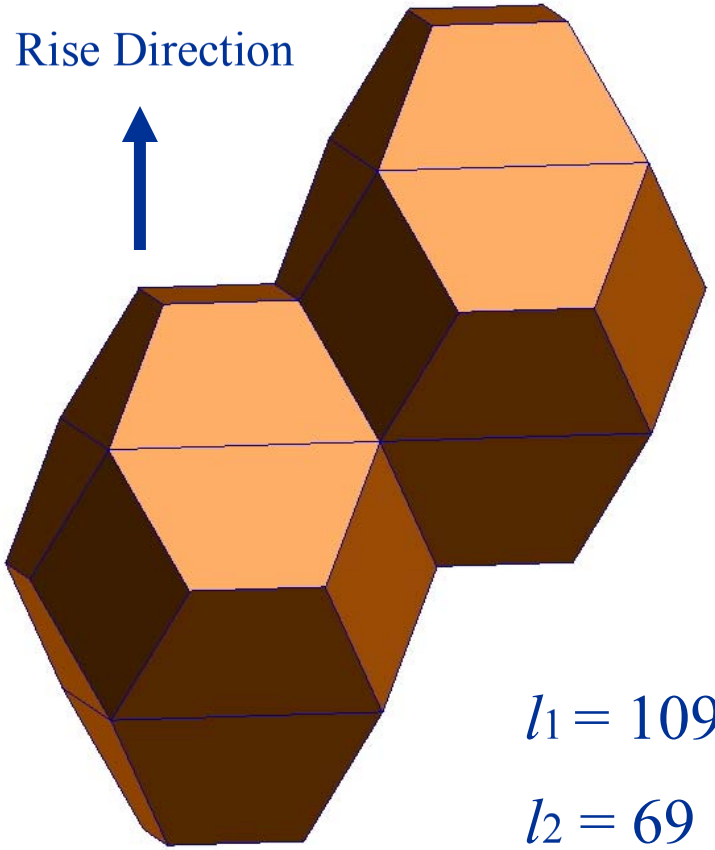

Packs to fill Volume

$l_1 = 109\ \mu m$

$l_2 = 69\ \mu m$

$l_3 = 39\ \mu m$

$l_4 = 28\ \mu m$

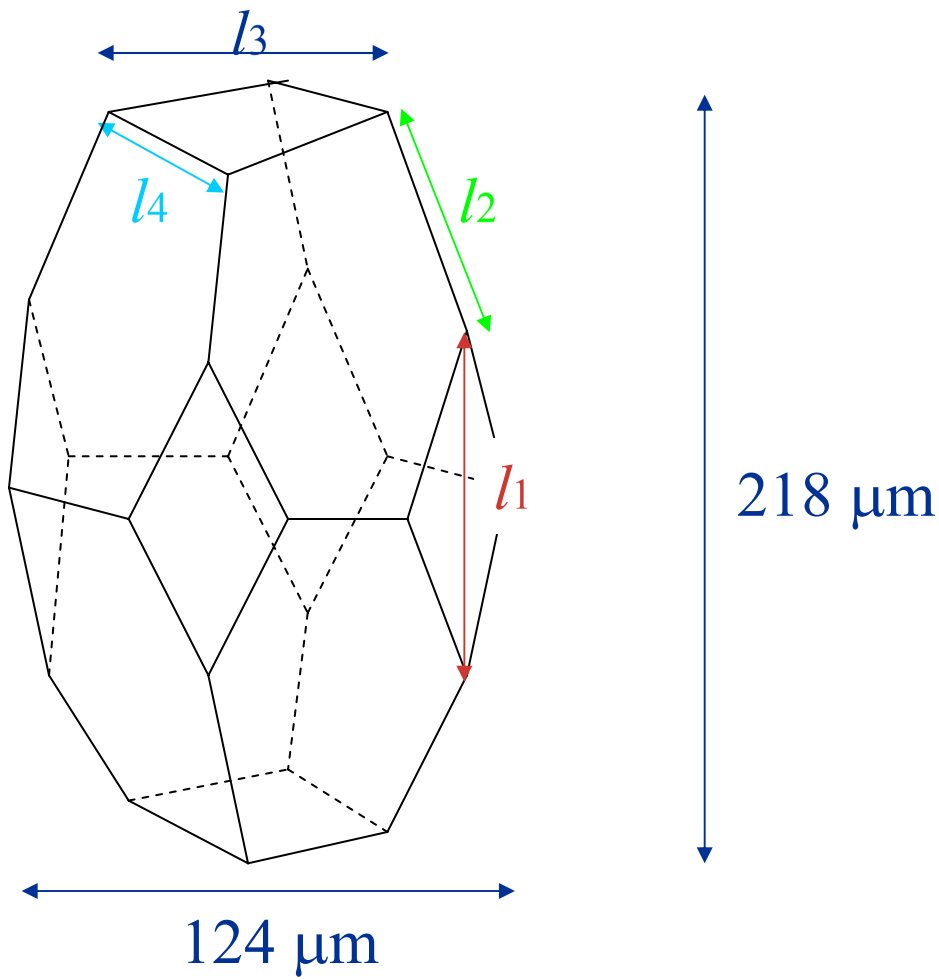

BX-265 Cell Dimensions

- Edges are solid, triangular beams.

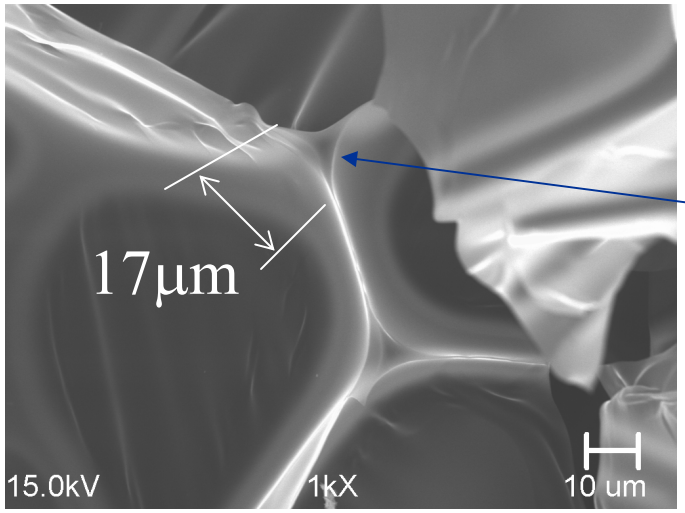

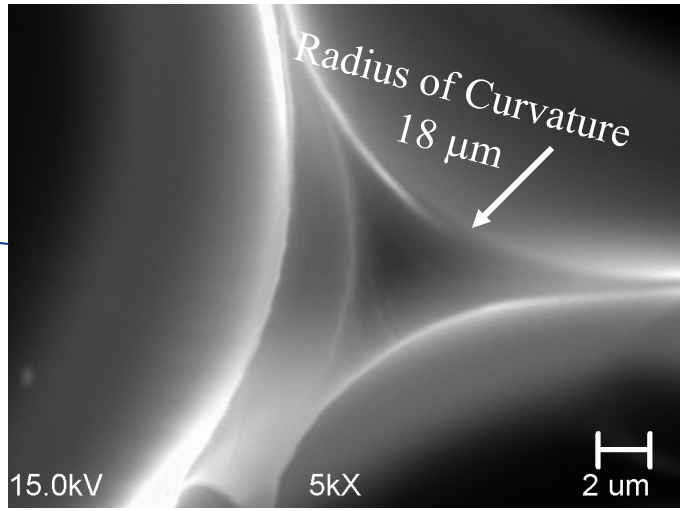

Triangular edges are 17 μm in width with average radii of 18 μm

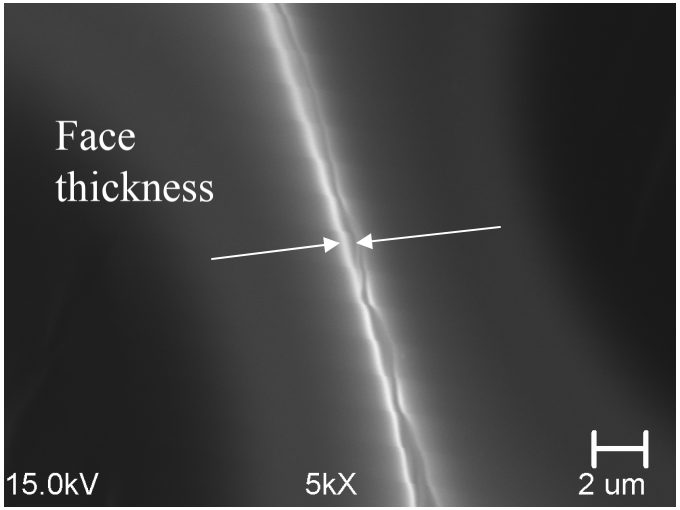

Faces are thin membranes 0.1<t<1.0 μm

Symmetry

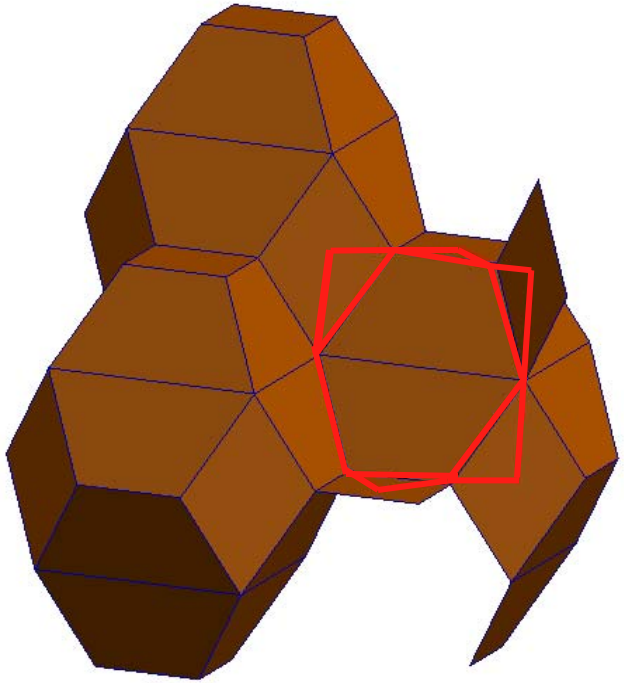

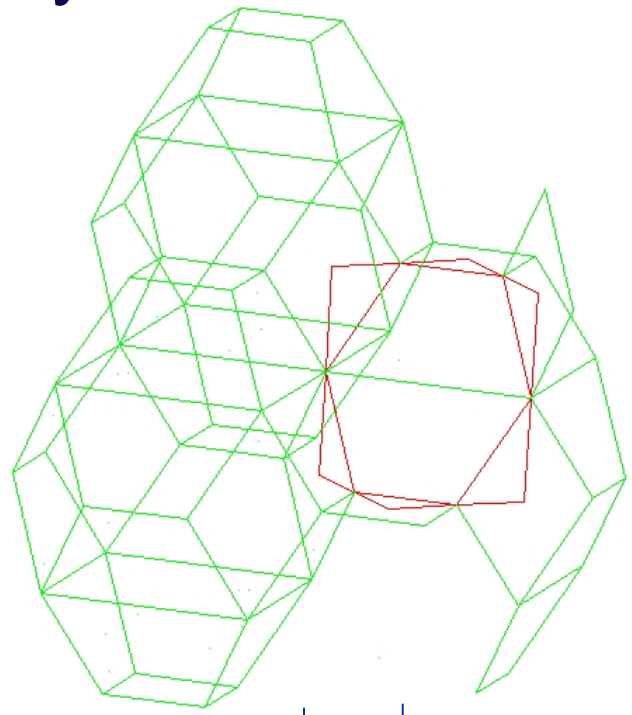

Cell Aspect Ratio
(Cell Length/Cell Width)

Top View
Normal to Rise

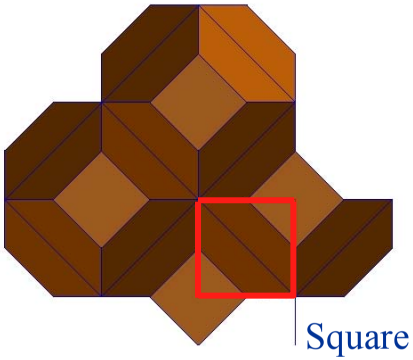

Square section

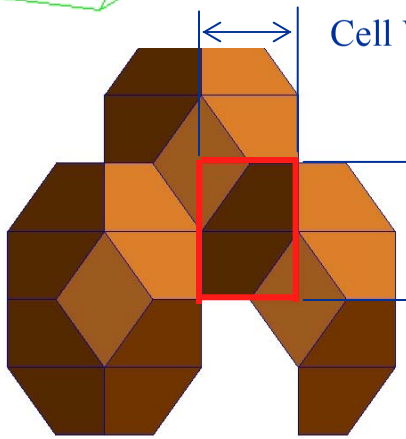

Cell Width

Rectangular section

Cell Length

Side View
Rise/In-plane

Finite Element Mesh for 1/8th Symmetry

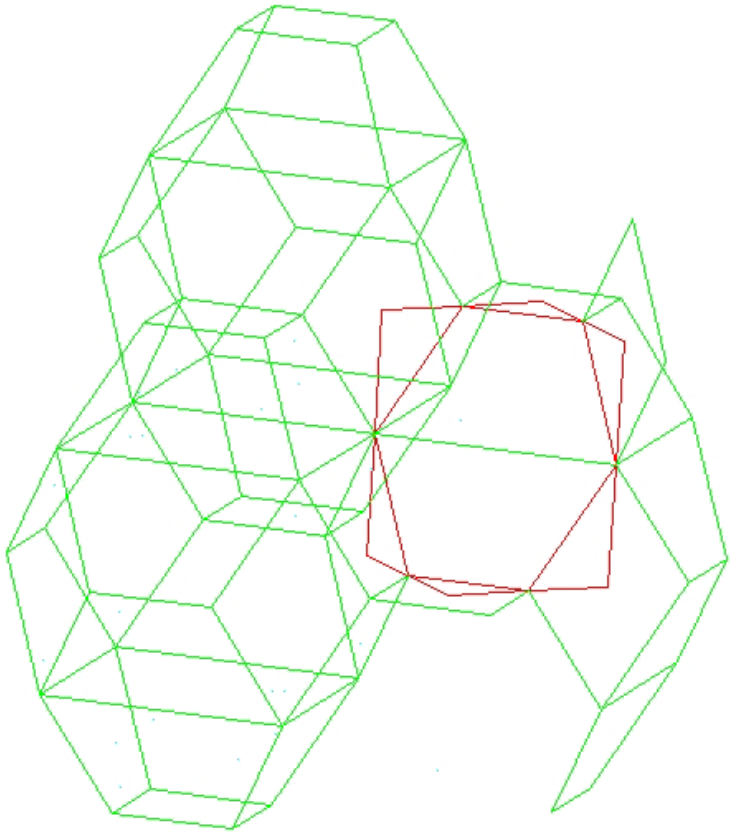

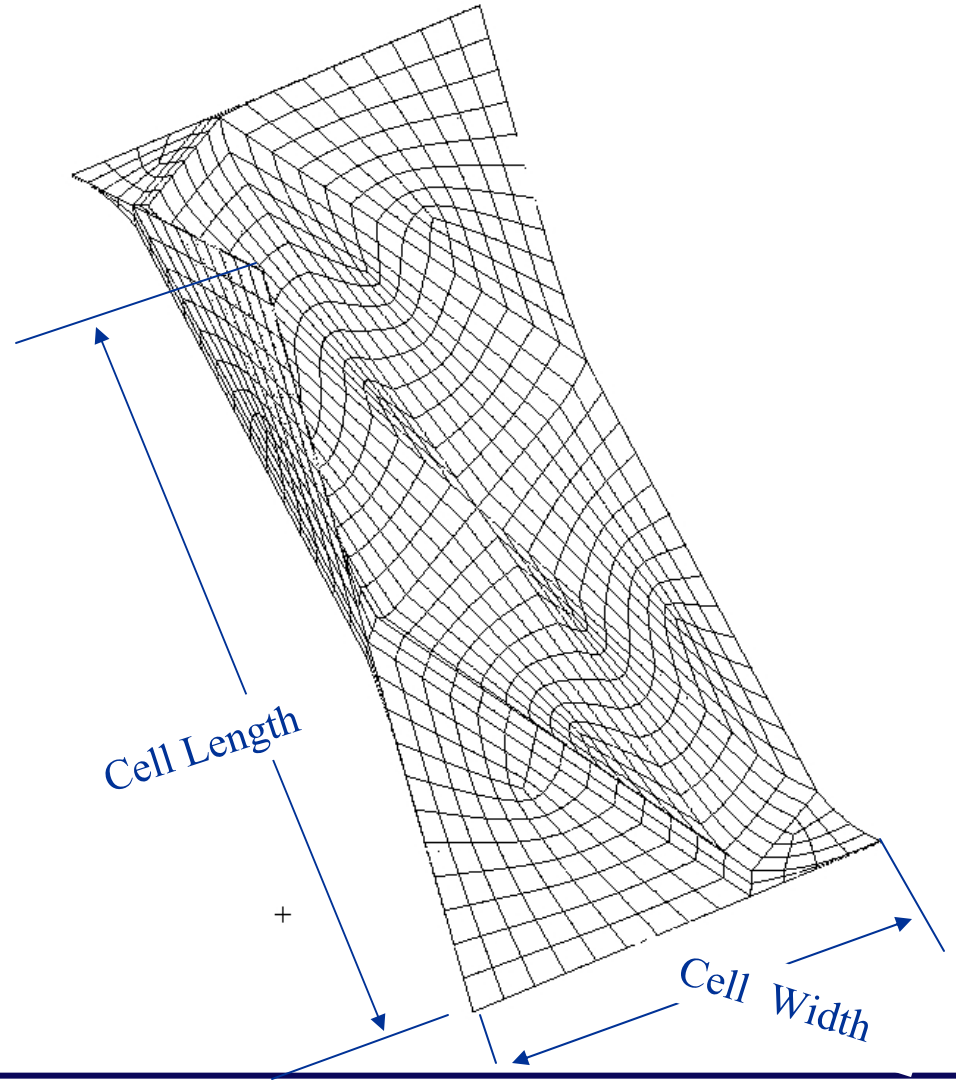

Finite Element Mesh for 1/8th Symmetry

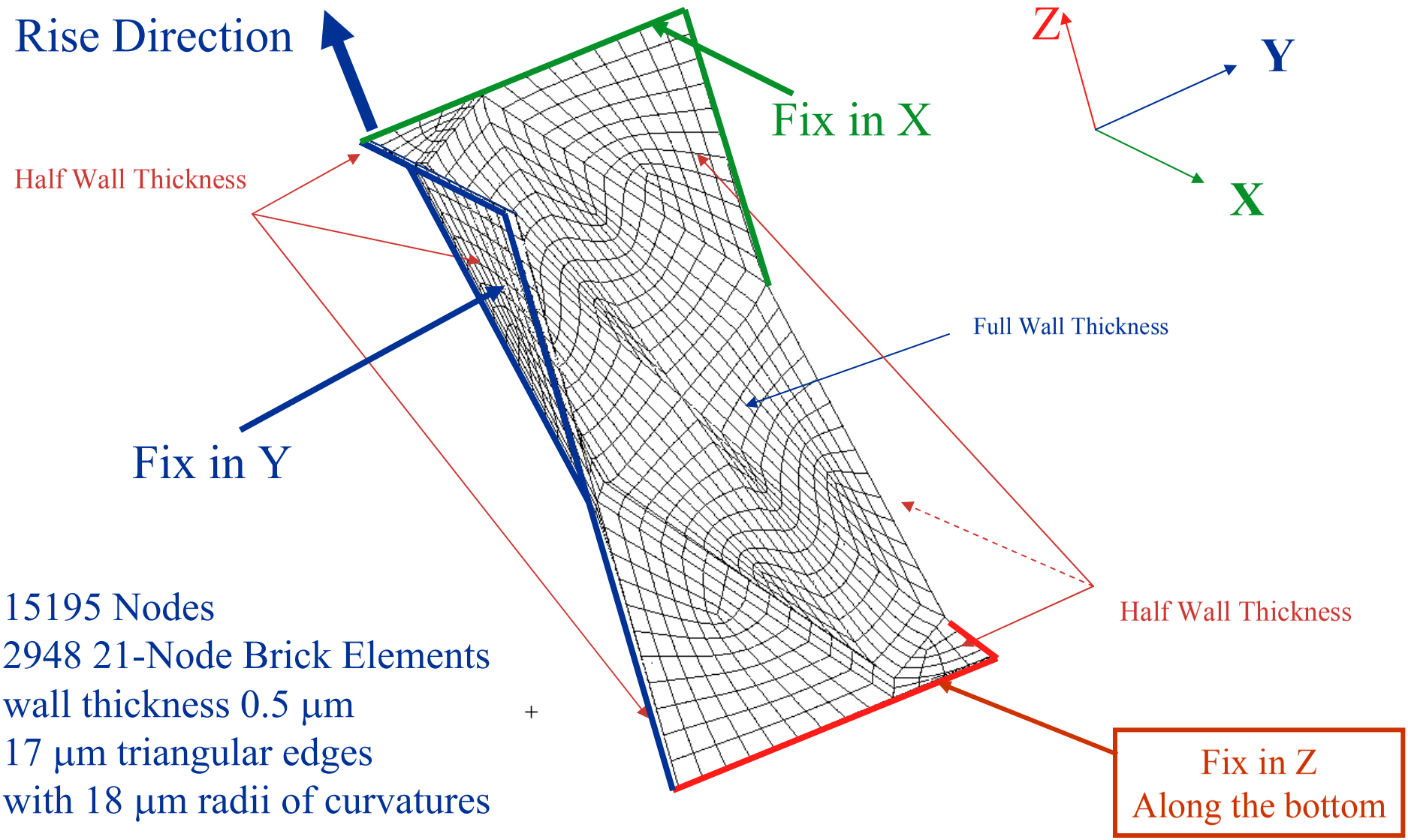

15195 Nodes
2948 21-Node Brick Elements
wall thickness 0.5 μm
17 μm triangular edges
with 18 μm radii of curvatures

Maximum Principal Stress for loading in the rise direction BX-265

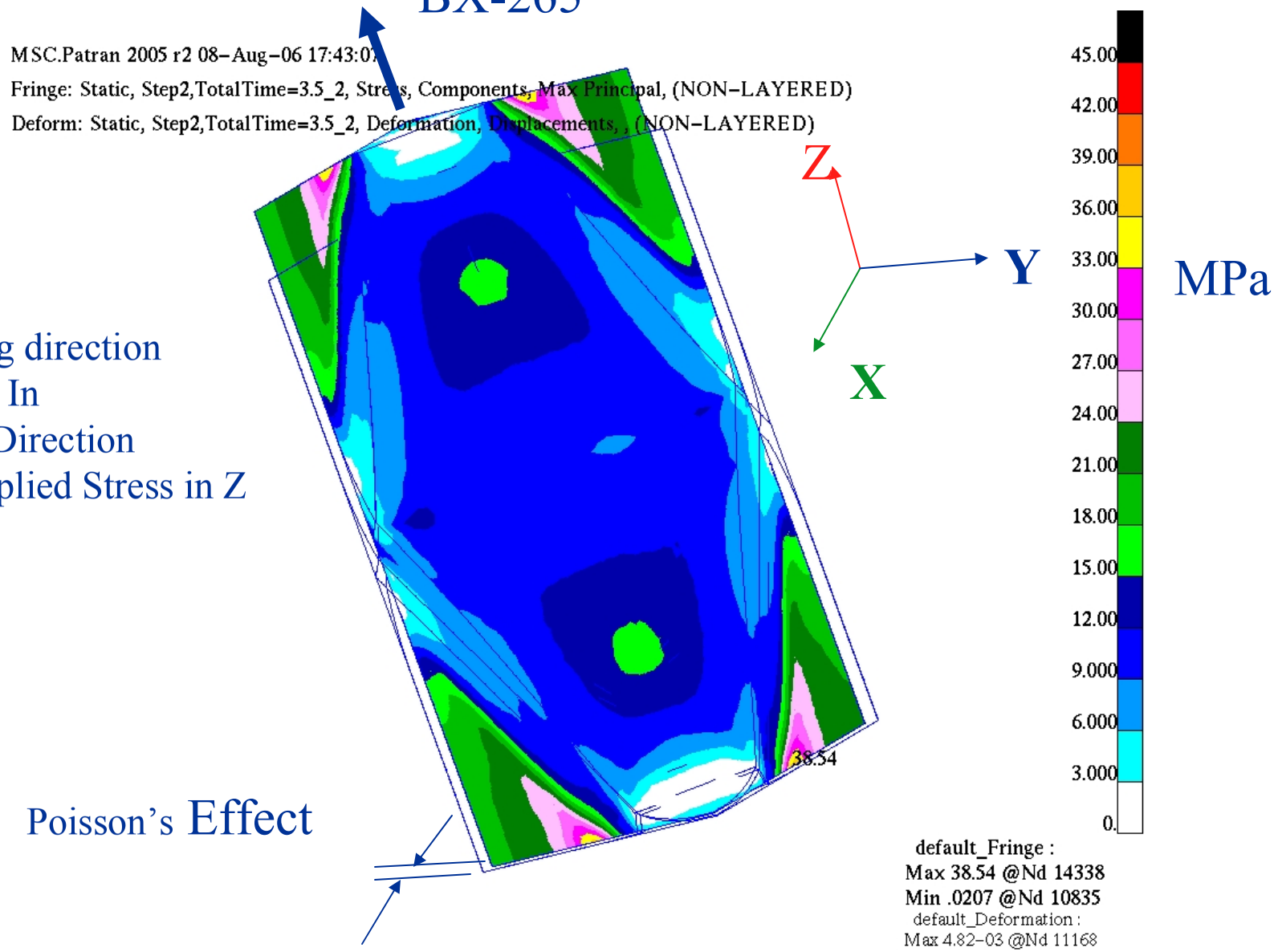

Loading direction
In
Rise Direction
0.31 MPa applied Stress in Z

Poisson's Effect

Maximum Principal Stress for in-plane loading BX-265

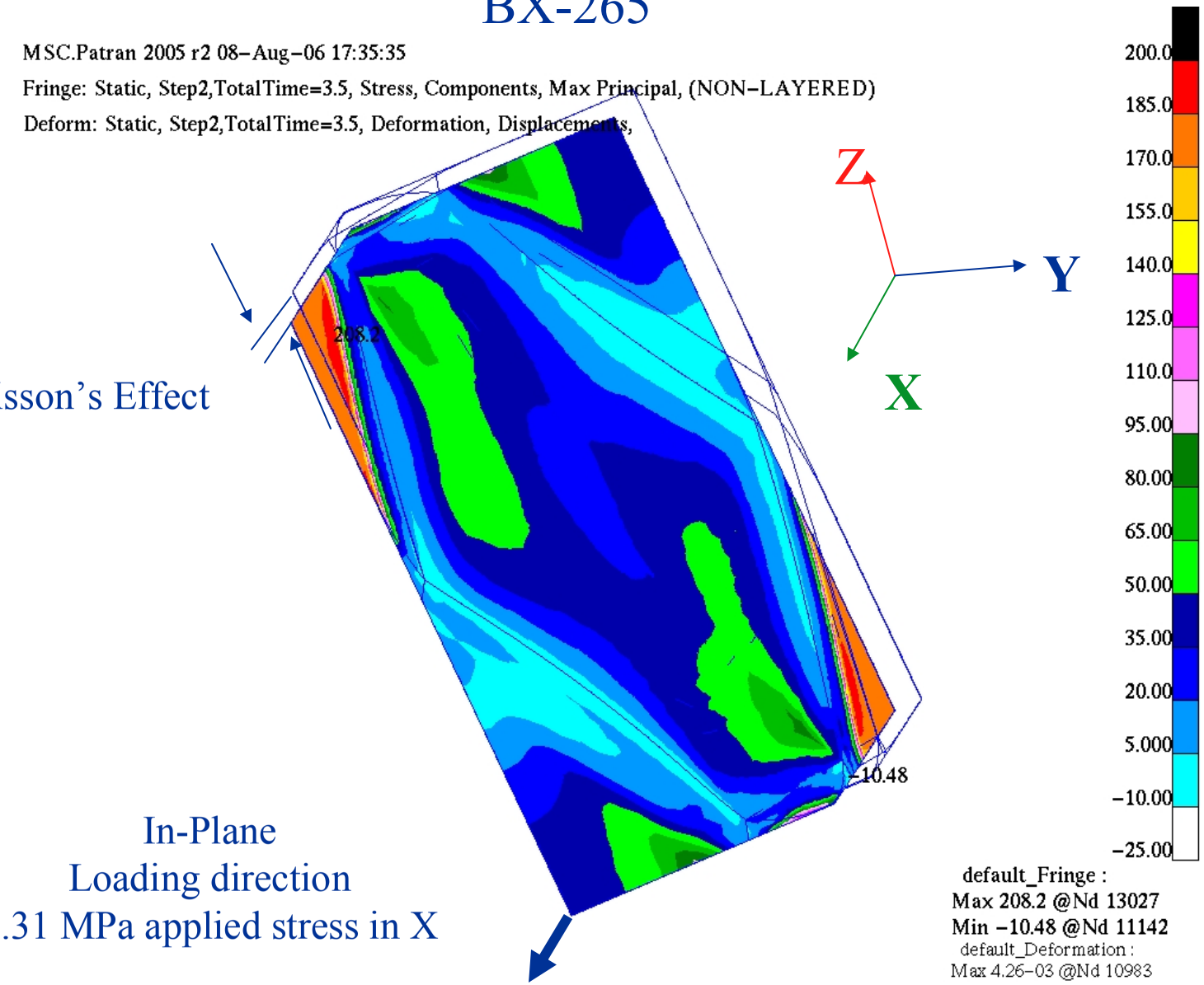

MPa

Poisson's Effect

In-Plane
Loading direction
0.31 MPa applied stress in X

Calibration of BX-265 Stress/Strain Curve

BX-265 @ room temperature

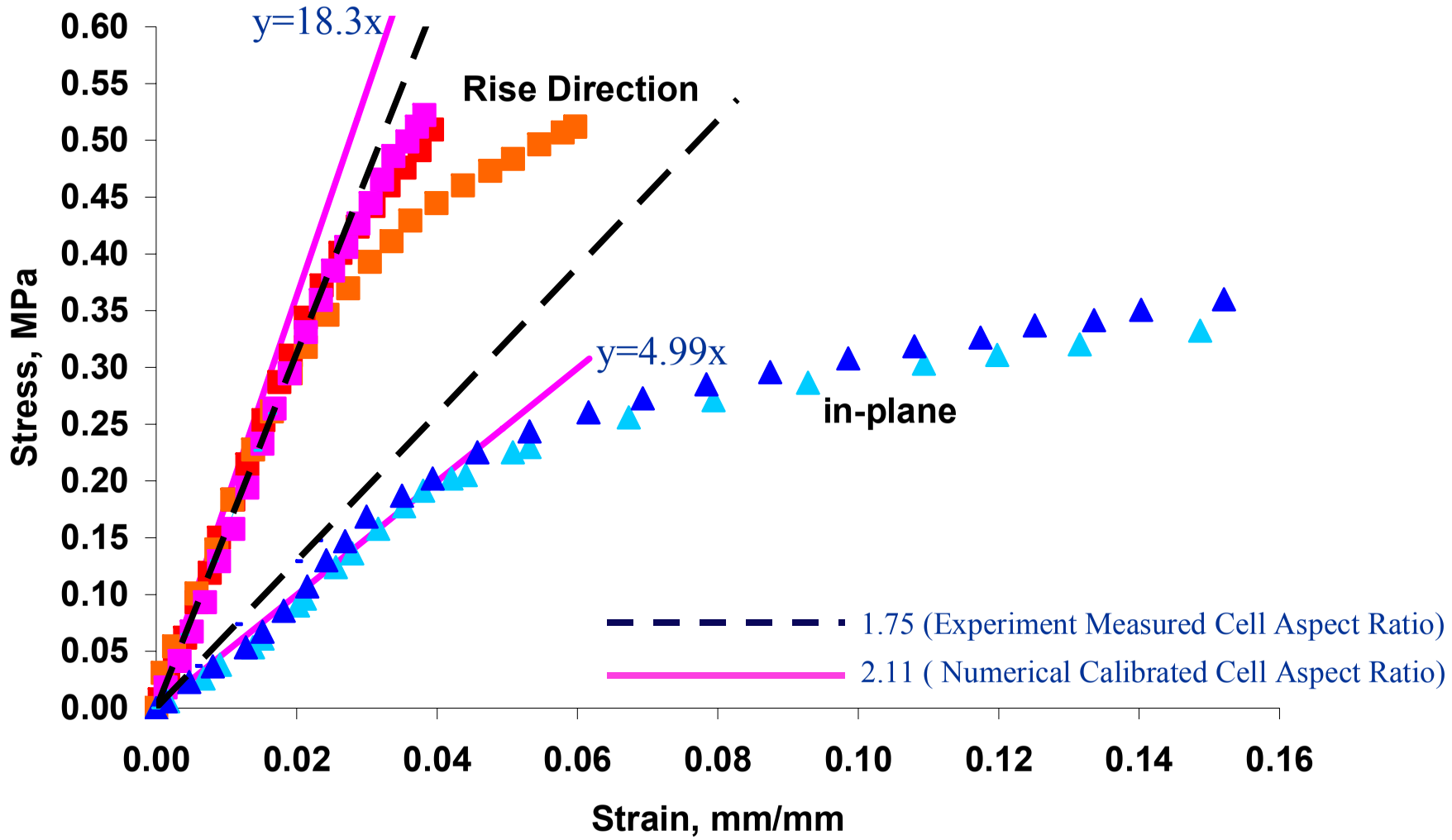

Experimental data courtesy of LMSSC External Tank Return to Flight, Fracture Toughness: Phase 2 (Kristin Morgan)

Effects of Solid Poisson's' Ratio on the Foam Stress/Strain Curve

BX-265 @ room temperature

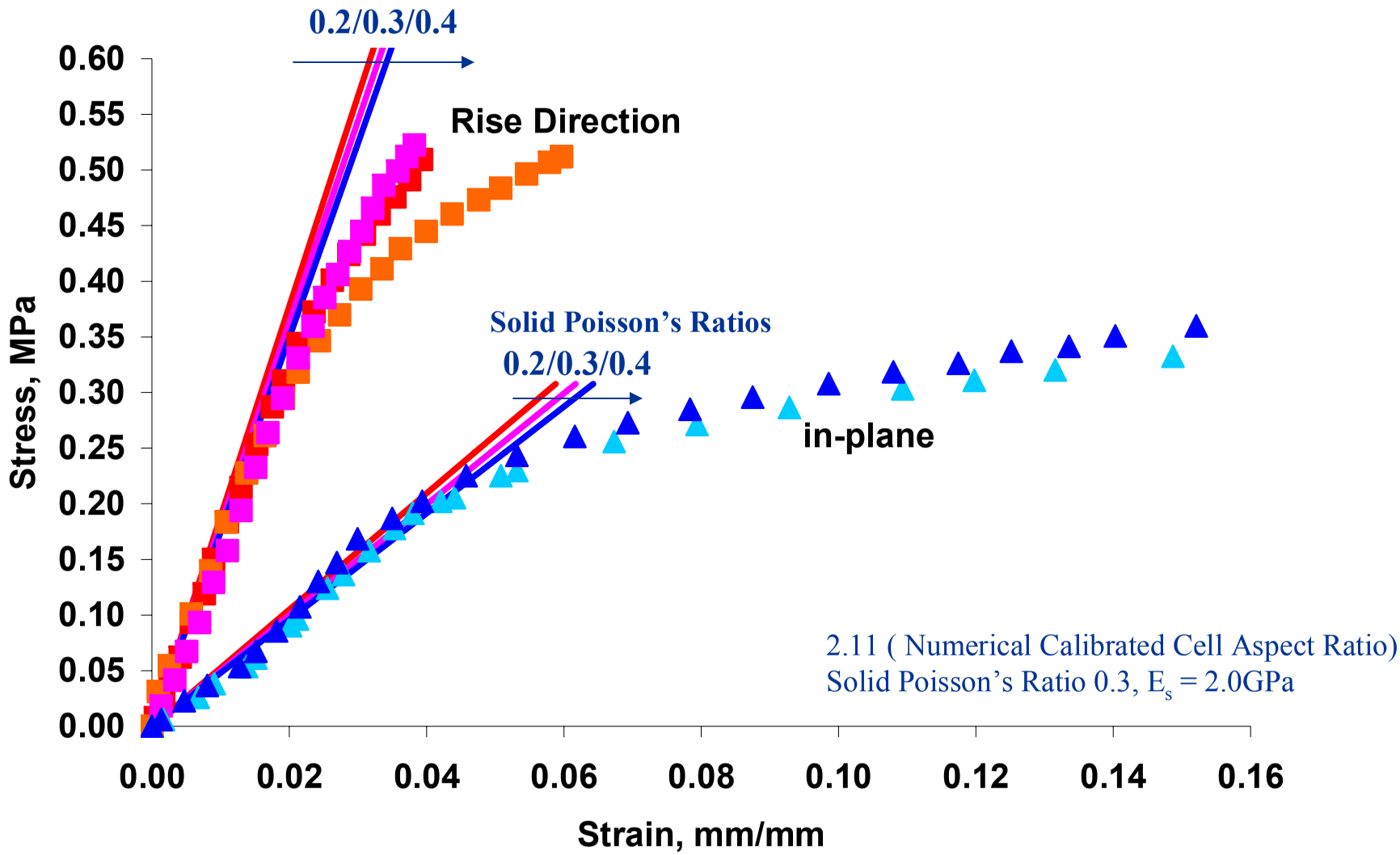

Experimental data courtesy of LMSSC External Tank Return to Flight, Fracture Toughness: Phase 2 (Kristin Morgan)

Calibration of BX-265 Stress/Strain Curve (-320 F)

BX-265 @ -195.6 C

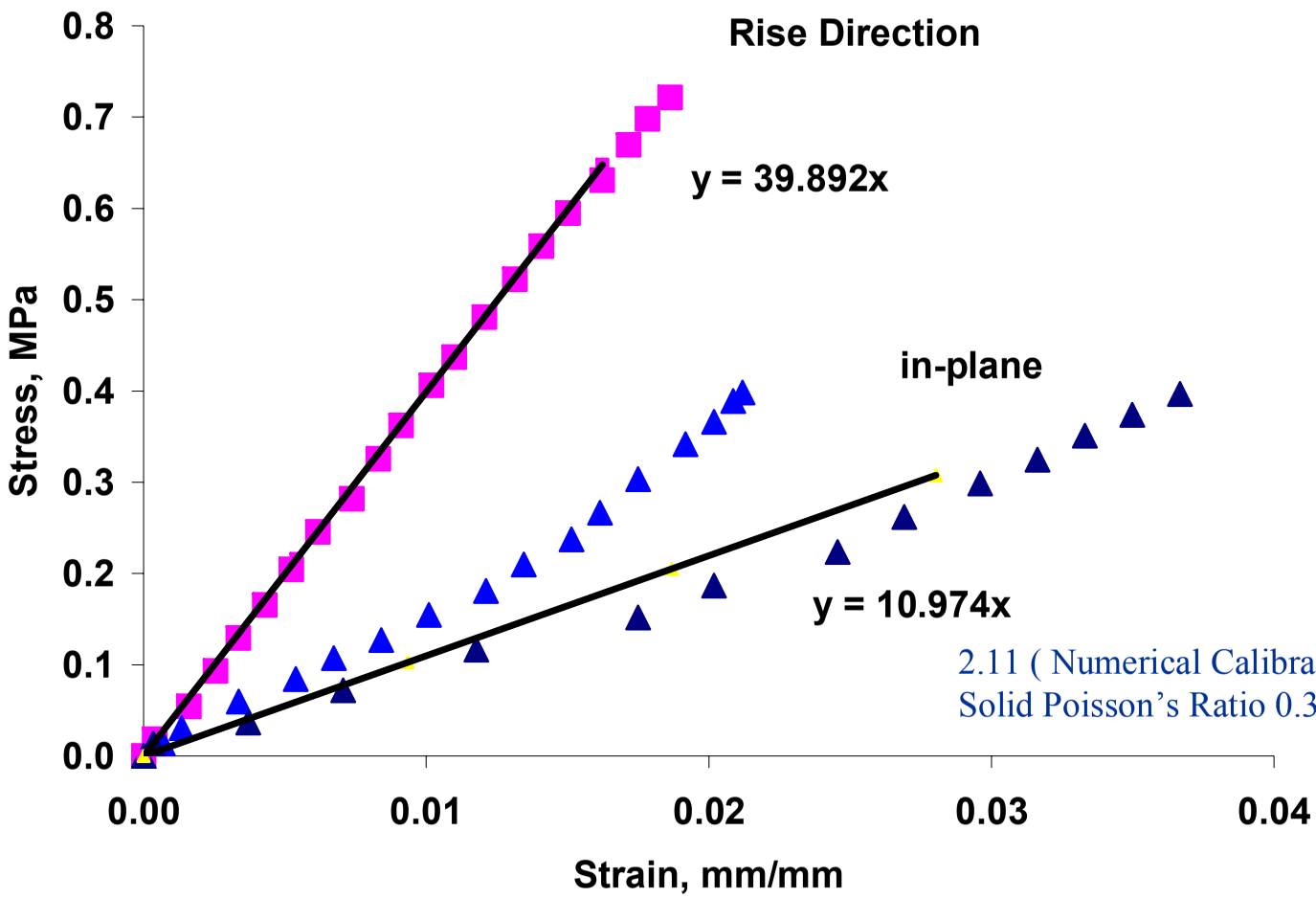

2.11 (Numerical Calibrated Cell Aspect Ratio)
Solid Poisson's Ratio 0.3, E_s = 4.4GPa

Experimental data courtesy of LMSSC External Tank Return to Flight, Fracture Toughness: Phase 2 (Kristin Morgan)

Calibration of BX-265 Stress/Strain Curve (-420 F)

BX-265 @ -251 C

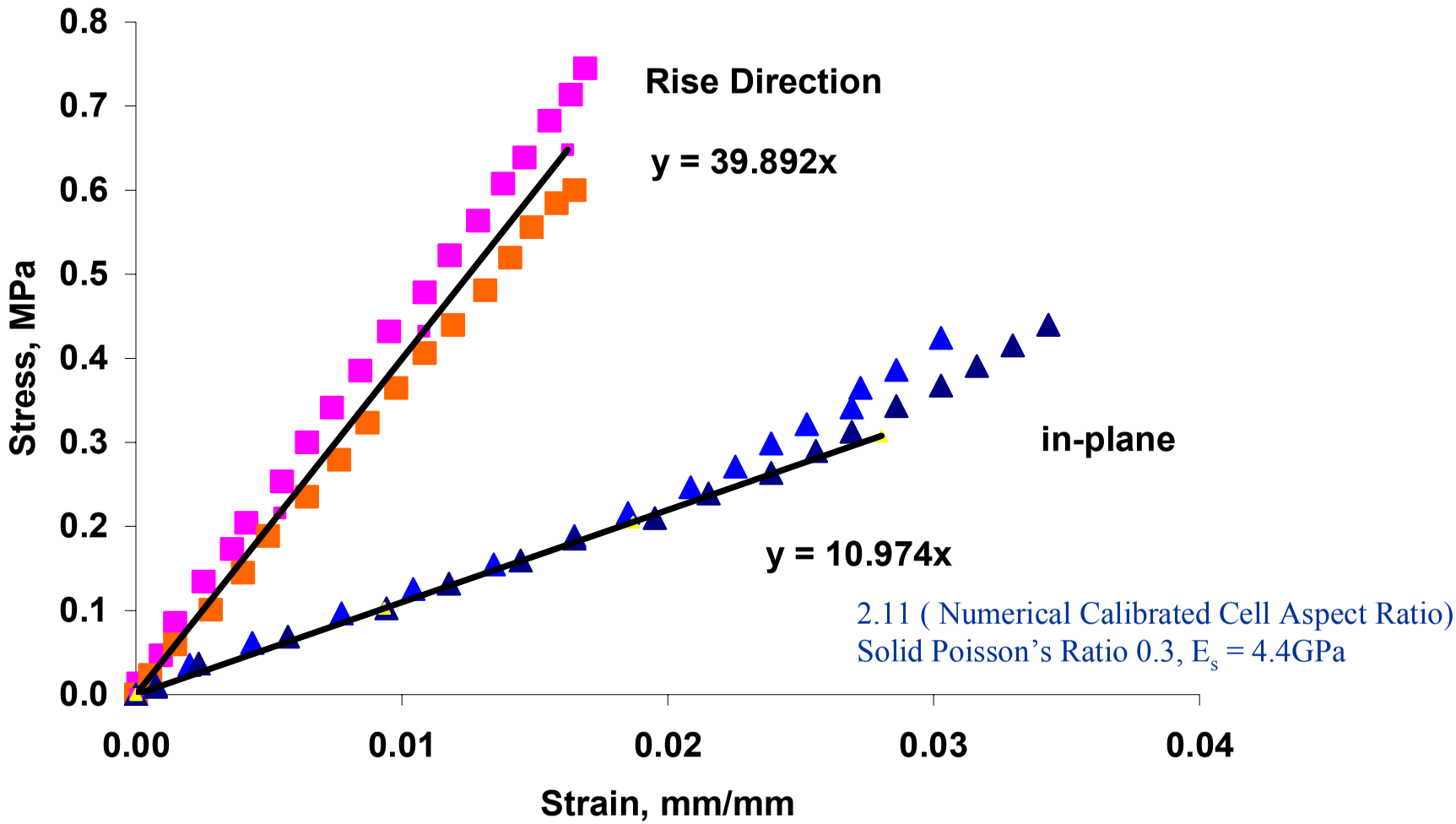

Experimental data courtesy of LMSSC External Tank Return to Flight, Fracture Toughness: Phase 2 (Kristin Morgan)

Calibration of NCFI Stress/Strain Curve (RT)

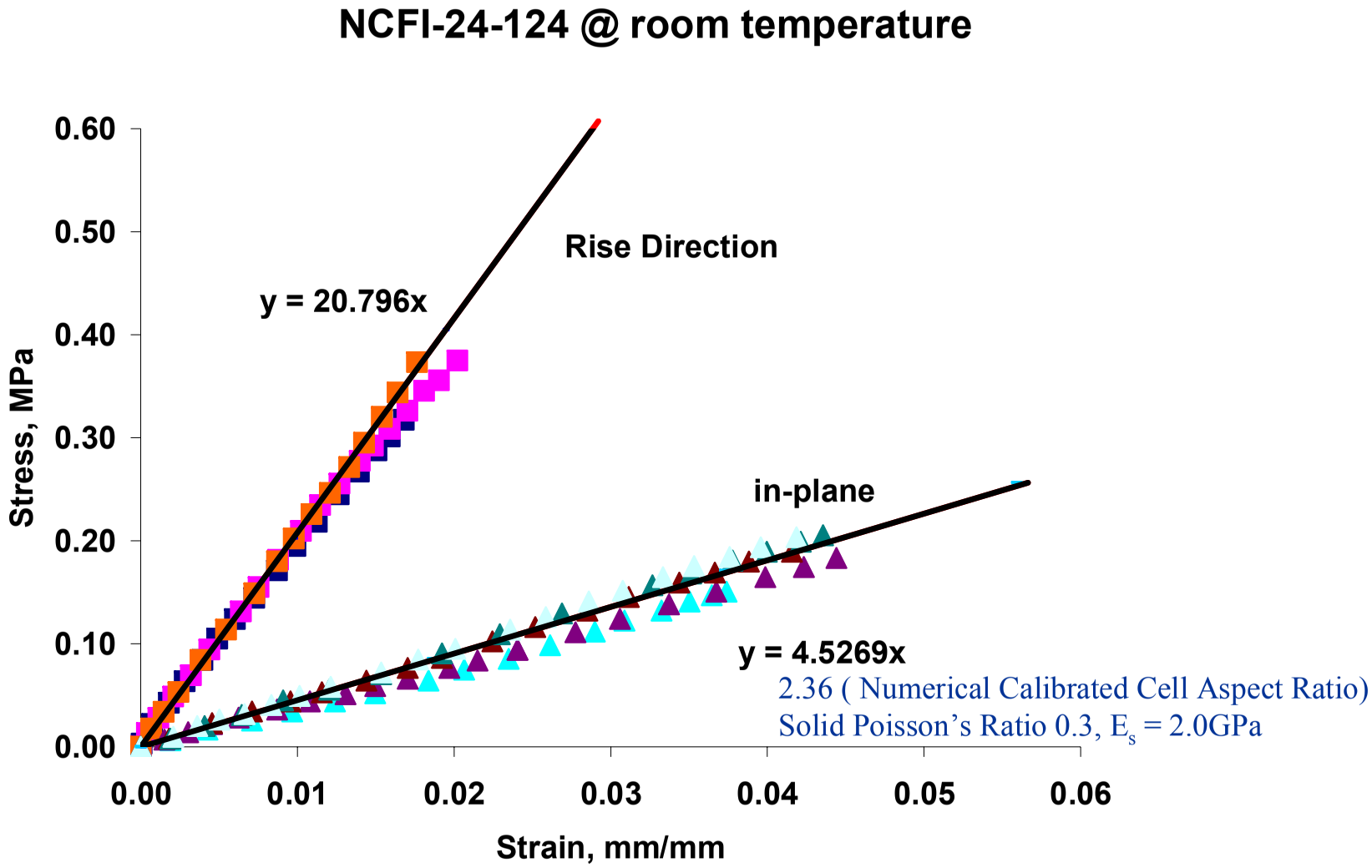

Experimental data courtesy of LMSSC External Tank Return to Flight, Fracture Toughness: Phase 2 (Kristin Morgan)

Calibration of NCFI Stress/Strain Curve (-320 F)

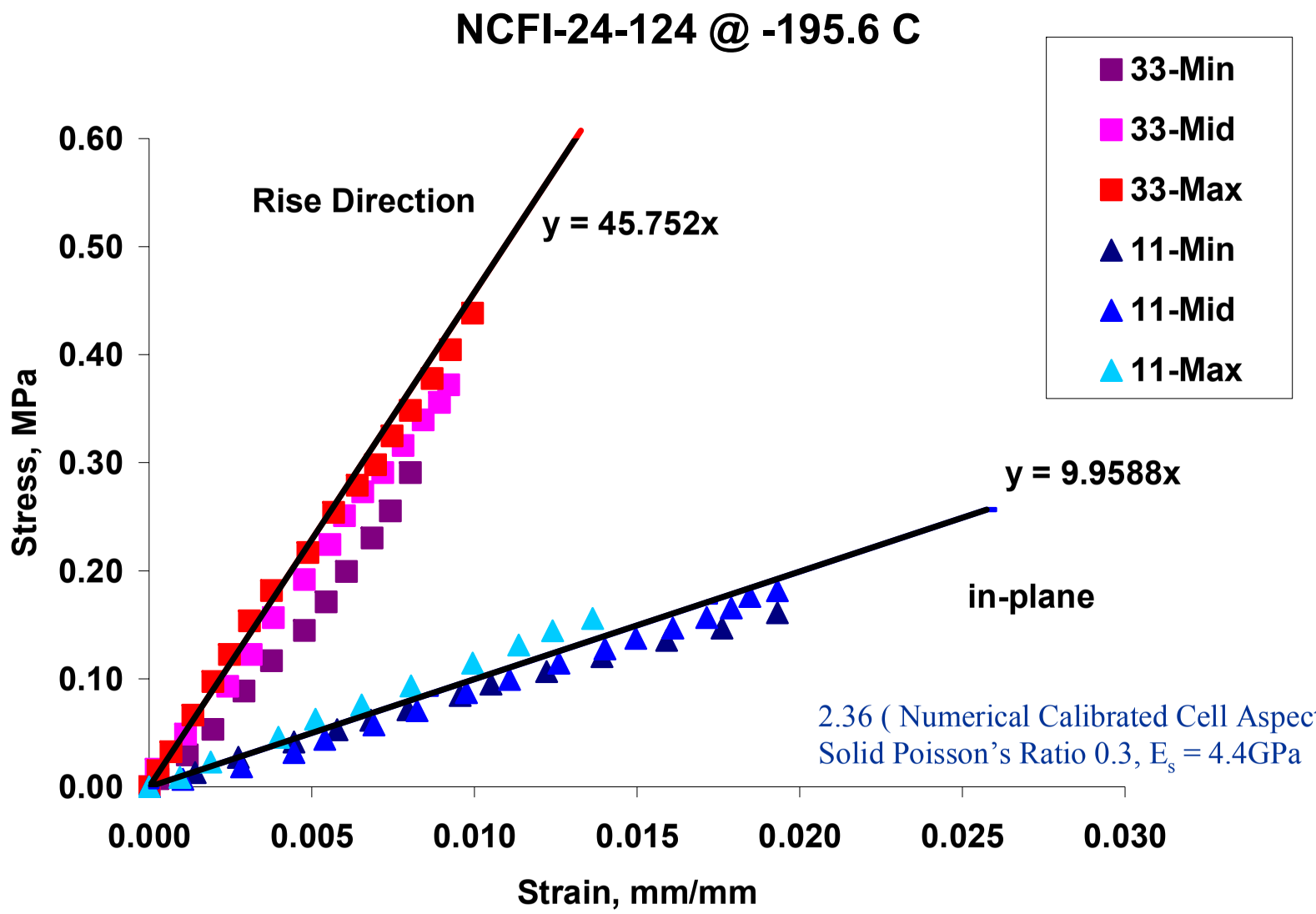

2.36 (Numerical Calibrated Cell Aspect Ratio)
Solid Poisson's Ratio 0.3, E_s = 4.4GPa

Experimental data courtesy of LMSSC External Tank Return to Flight, Fracture Toughness: Phase 2 (Kristin Morgan)

Calibration of NCFI Stress/Strain Curve (-420 F)

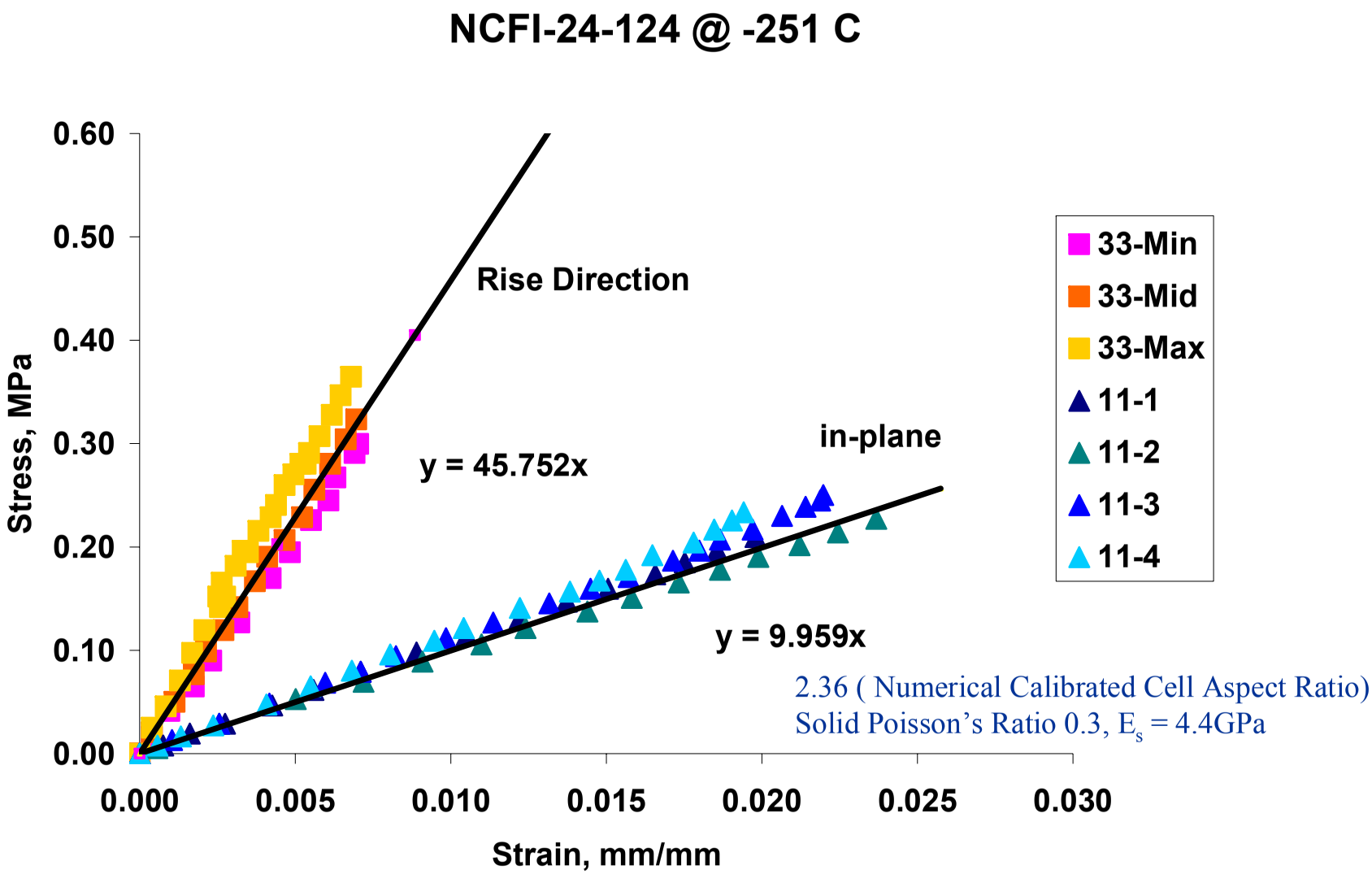

2.36 (Numerical Calibrated Cell Aspect Ratio)
Solid Poisson's Ratio 0.3, E_s = 4.4GPa

Experimental data courtesy of LMSSC External Tank Return to Flight, Fracture Toughness: Phase 2 (Kristin Morgan)

Calibration of PDL Stress/Strain Curve (RT)

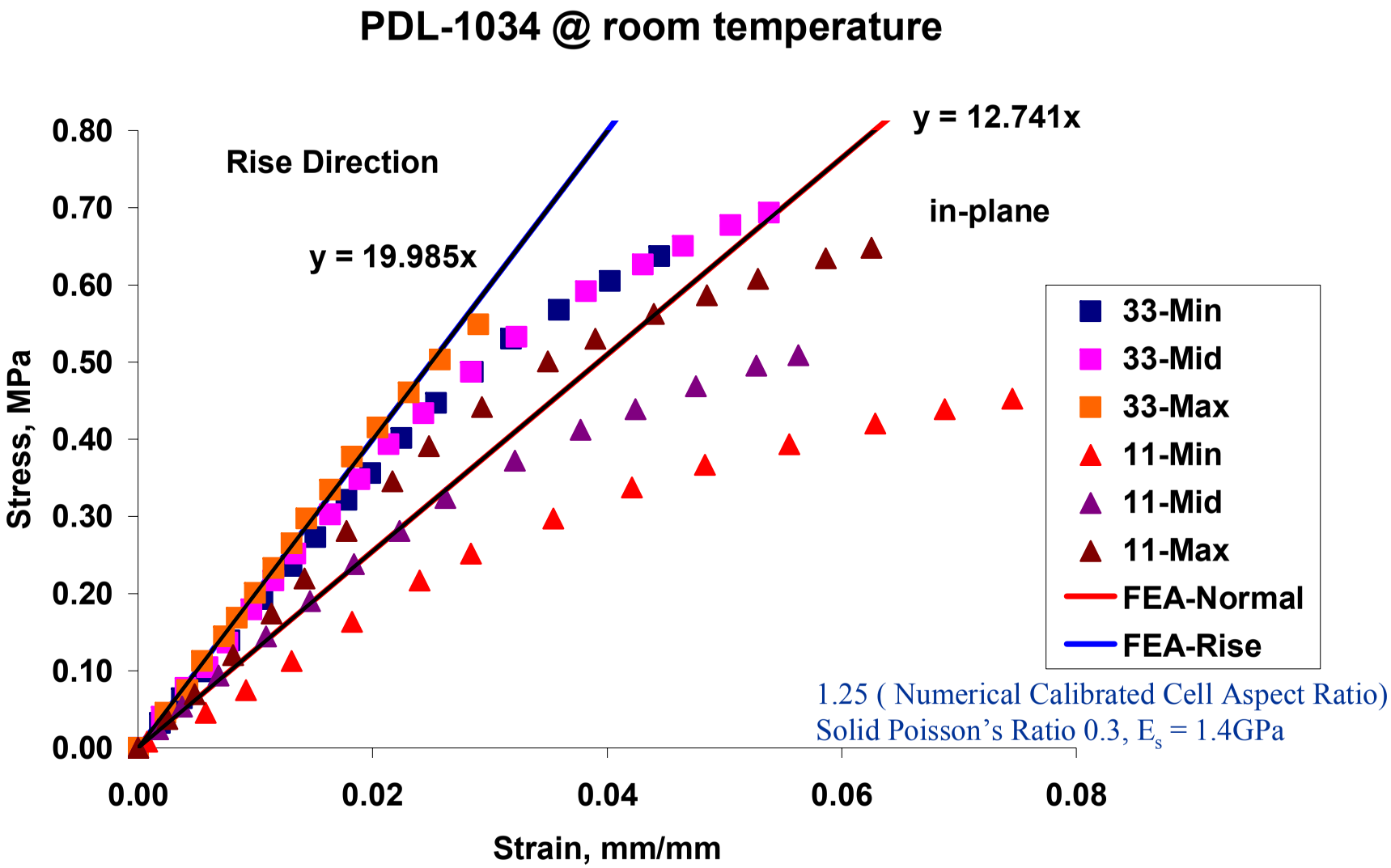

1.25 (Numerical Calibrated Cell Aspect Ratio)
Solid Poisson's Ratio 0.3, E_s = 1.4GPa

Experimental data courtesy of LMSSC External Tank Return to Flight, Fracture Toughness: Phase 2 (Kristin Morgan)

Calibration of PDL Stress/Strain Curve (-320 F)

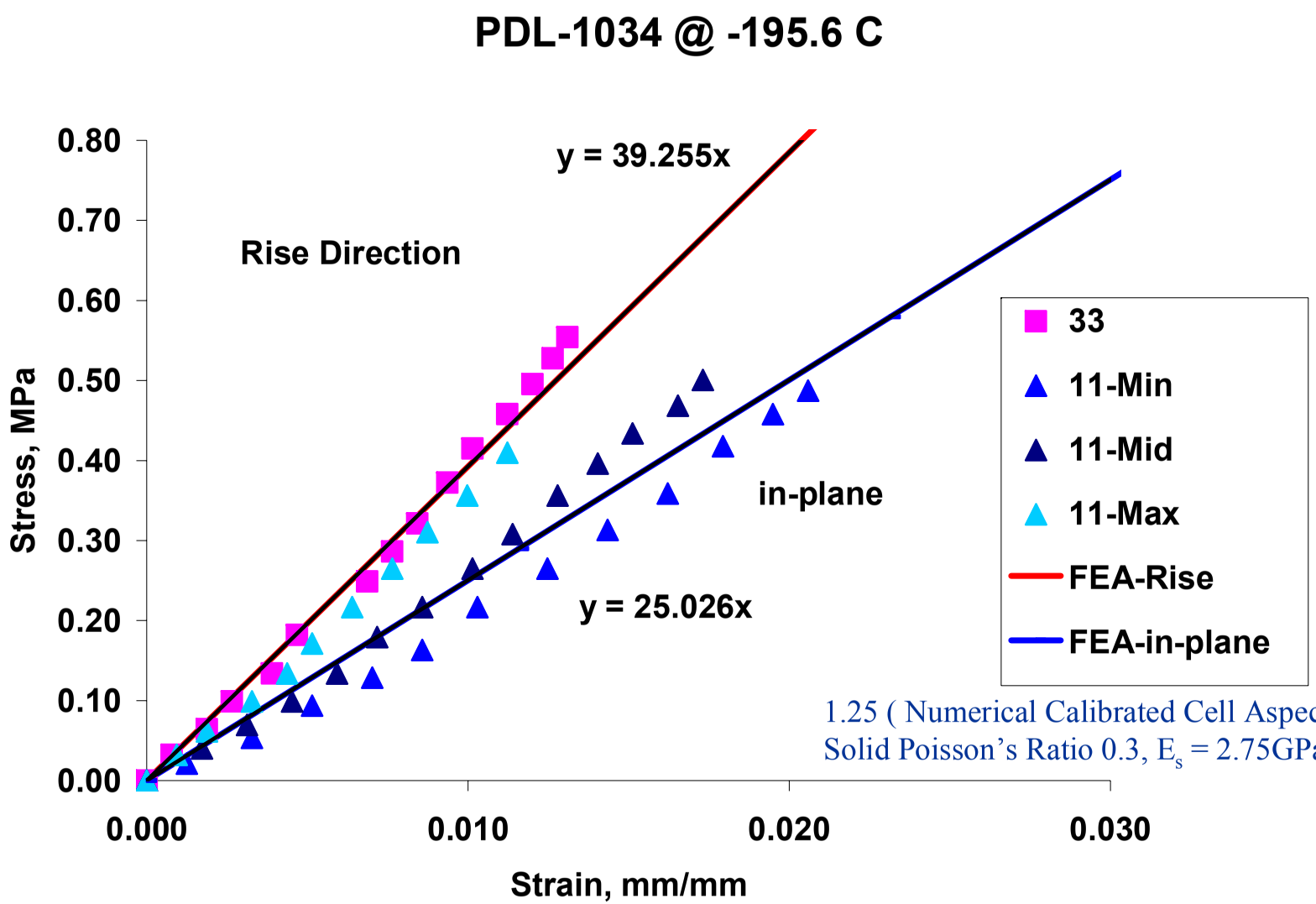

1.25 (Numerical Calibrated Cell Aspect Ratio)
Solid Poisson's Ratio 0.3, E_s = 2.75GPa

Experimental data courtesy of LMSSC External Tank Return to Flight, Fracture Toughness: Phase 2 (Kristin Morgan)

Calibration of PDL Stress/Strain Curve (-420 F)

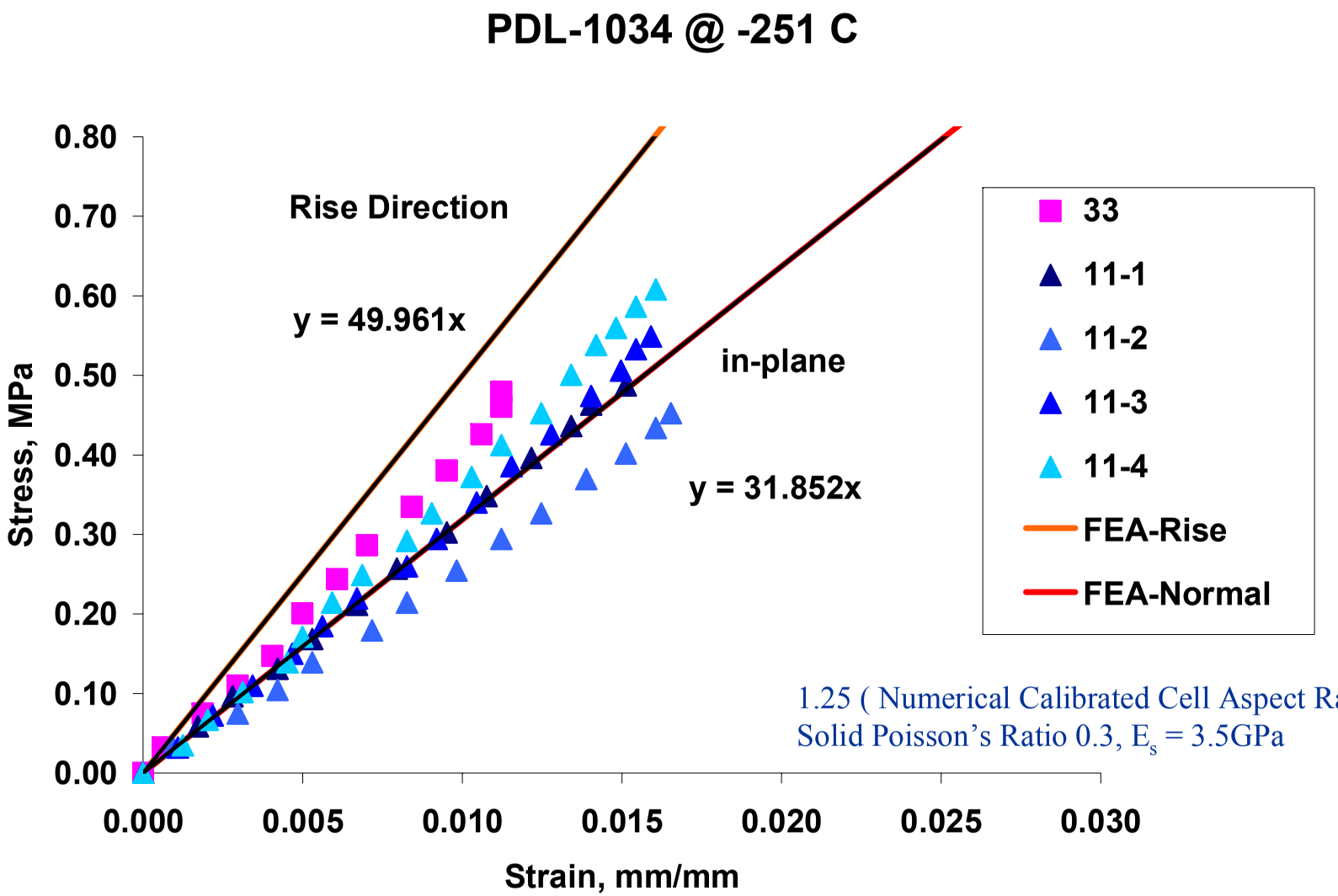

1.25 (Numerical Calibrated Cell Aspect Ratio)
Solid Poisson's Ratio 0.3, E_s = 3.5GPa

Experimental data courtesy of LMSSC External Tank Return to Flight, Fracture Toughness: Phase 2 (Kristin Morgan)

		Average Unit Cell			Solid			
		Length	Width	Aspect Ratio	Poisson's Ratio	Modulus, E_s		
						@ RT	@ -195.6 C	@ -195.6 C
		μm	μm			GPa	GPa	GPa
Calibrated	BX-265	262	124	2.11	0.3	2.0	4.4	4.4
	NCFI	236	100	2.36	0.3	2.0	4.4	4.4
	PDL	294	235	1.25	0.3	1.4	2.75	3.5
Measured	BX-265	218	124	1.76				

Foam Effective Elastic Properties

BX-265

Temp (C)	E11 (MPa)	E22 (MPa)	E33 (MPa)	nu12	nu13	nu23
-251	10.97	10.97	39.89	0.488	0.143	0.143
-196	10.97	10.97	39.89	0.488	0.143	0.143
24	4.99	4.99	18.13	0.488	0.143	0.143

NCFI

Temp (C)	E11 (MPa)	E22 (MPa)	E33 (MPa)	nu12	nu13	nu23
-251	9.96	9.96	45.75	0.528	0.114	0.114
-196	9.96	9.96	45.75	0.528	0.114	0.114
24	4.53	4.53	20.80	0.528	0.114	0.114

PDL

Temp (C)	E11 (MPa)	E22 (MPa)	E33 (MPa)	nu12	nu13	nu23
-253	31.85	31.85	49.96	0.362	0.249	0.249
-196	25.03	25.03	39.26	0.362	0.249	0.249
24	12.74	12.74	19.99	0.362	0.249	0.249

UTS of NCFI at RT

NCFI 24-124: Round 7" Dogbone Specimen

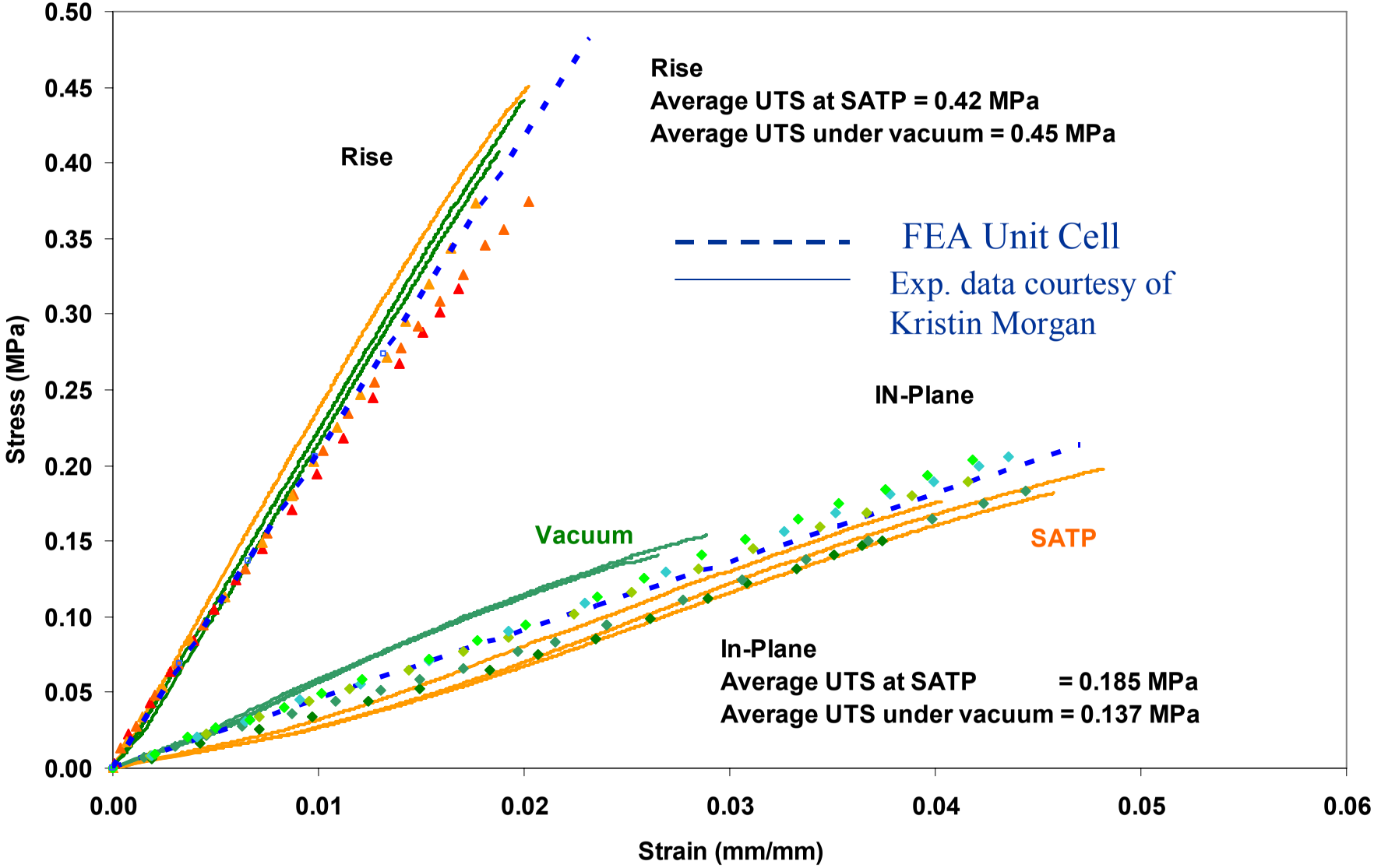

Symbols data LMSSC External Tank Return to Flight, Fracture Toughness: Phase 2 (Kristin Morgan)

Maximum Principal Stress for loading in the rise direction NCFI (1 atm)

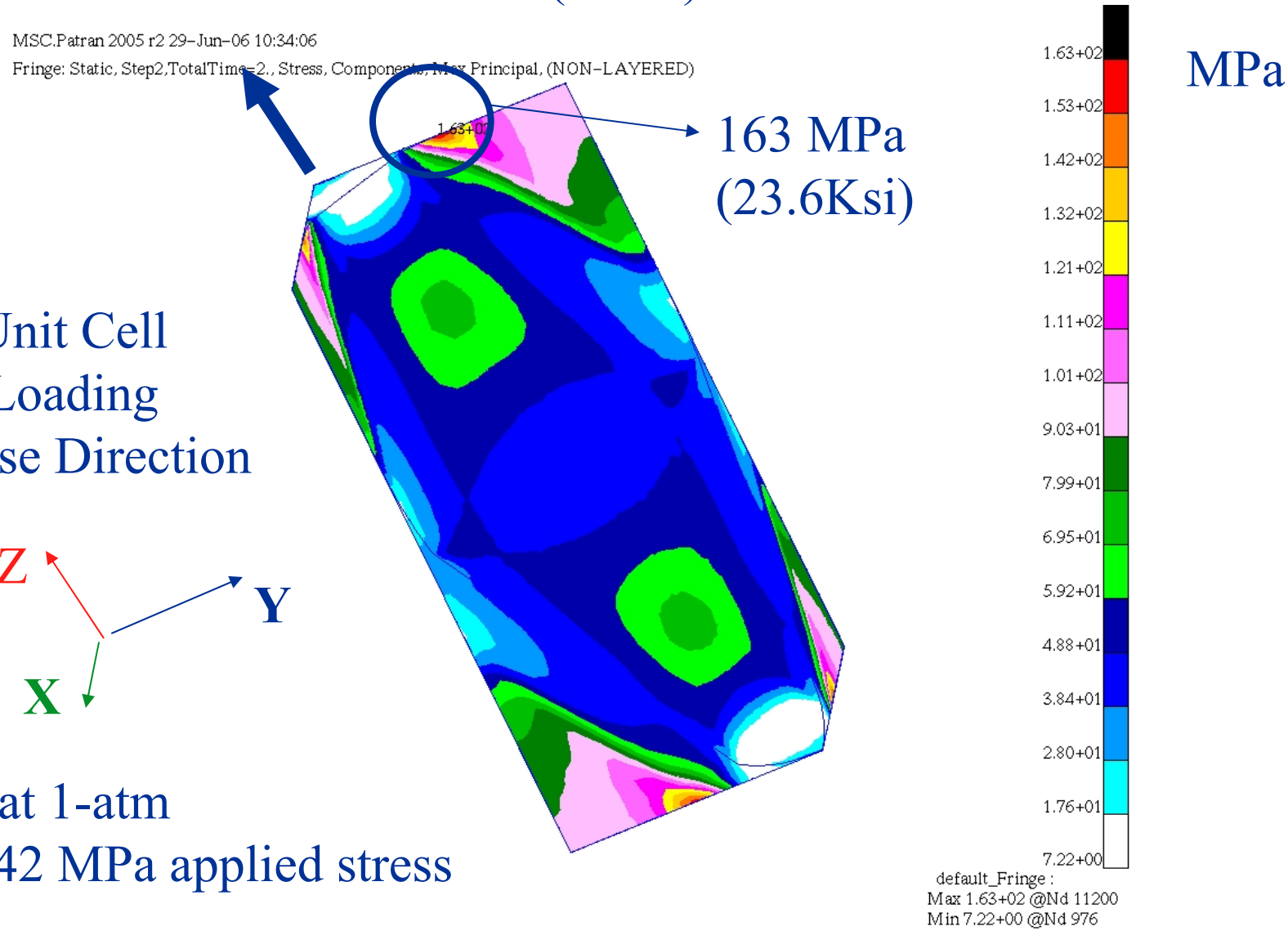

Unit Cell
Loading
In Rise Direction

Z
Y
X

Rise at 1-atm
@ 0.42 MPa applied stress

Maximum Principal Stress for loading in the in-plane direction NCFI (1 atm)

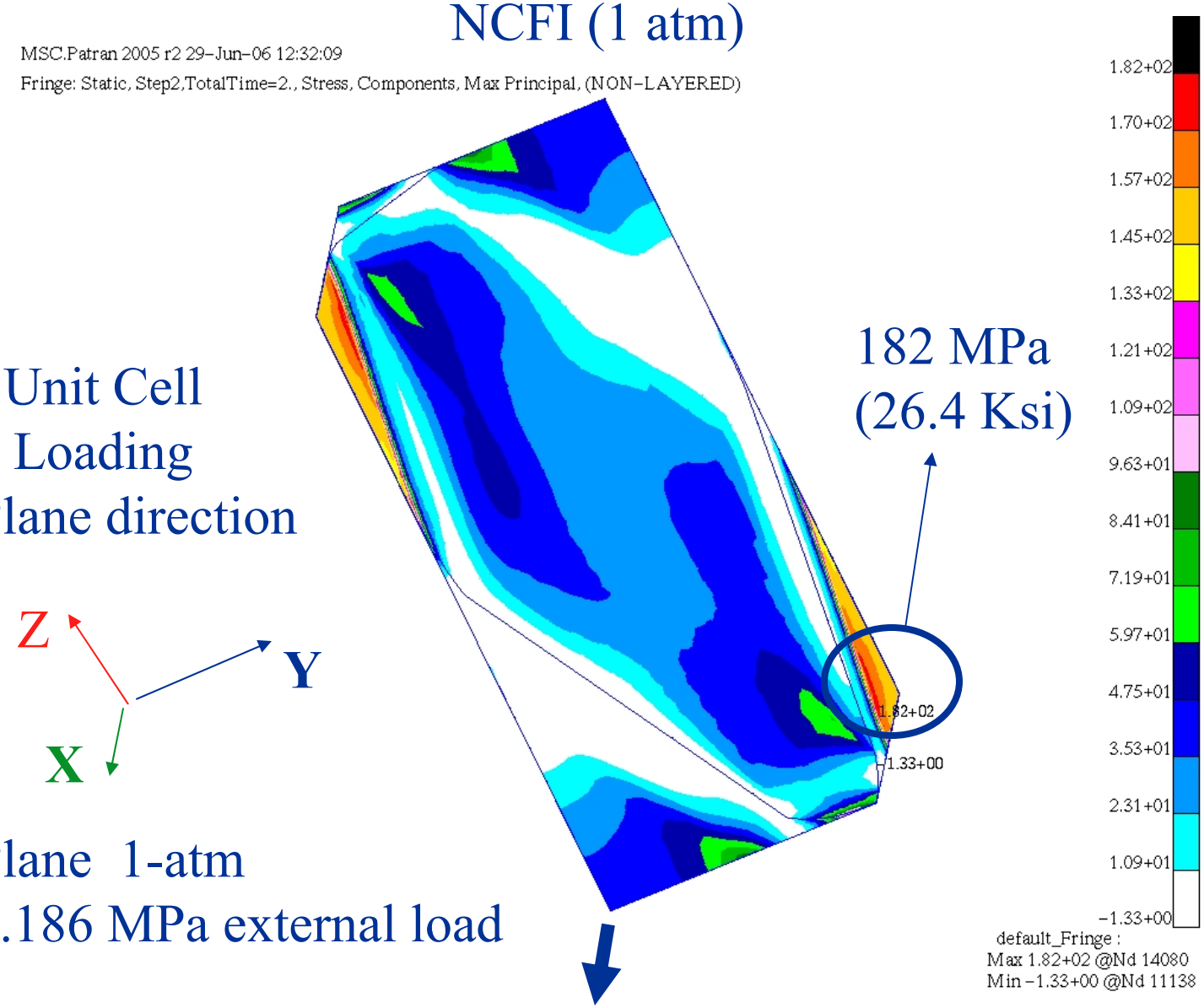

182 MPa
(26.4 Ksi)

MPa

Unit Cell
Loading
In-Plane direction

In-Plane 1-atm
@ 0.186 MPa external load

Maximum Principal Stress for loading in the rise direction NCFI (Vacuum Test)

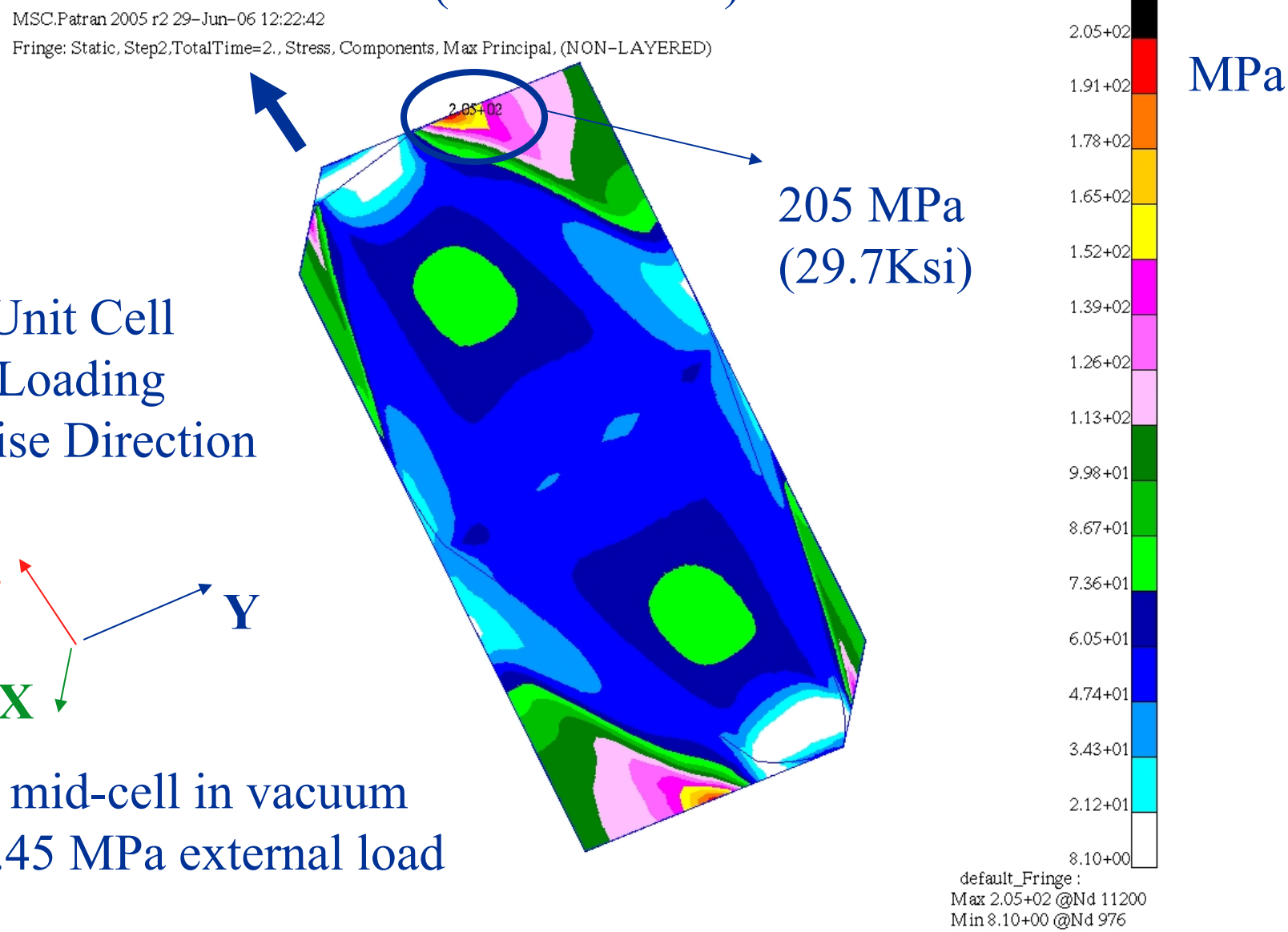

Unit Cell
Loading
In Rise Direction

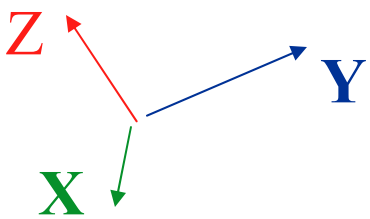

Rise mid-cell in vacuum
@ 0.45 MPa external load

Maximum Principal Stress for loading in the rise direction NCFI (Vacuum Test)

141 MPa
(20.5 Ksi)

Unit Cell
Loading
In-Plane direction
vacuum

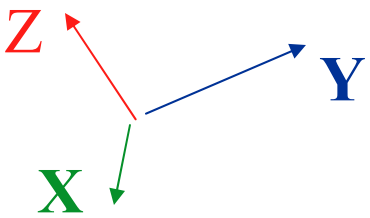

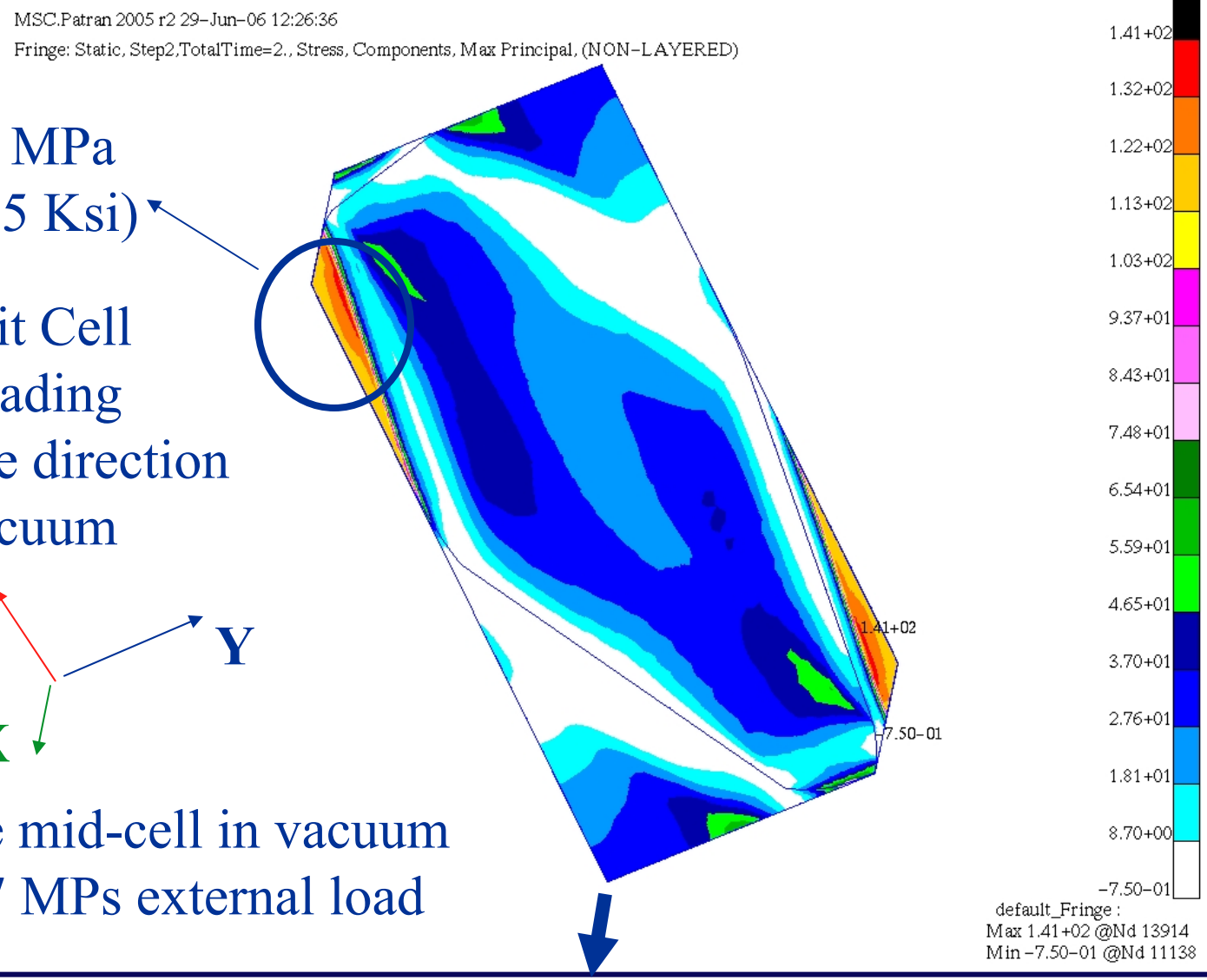

MPa

In-Plane mid-cell in vacuum
@ 0.127 MPs external load

NCFI, UTS		Applied Stress	Max. Principal
		MPa	MPa
Rise	SATM	0.42	169
In-Plane	SATM	0.186	182
Rise	Vacuum	0.45	205
In-Plane	Vacuum	0.127	141

Loading in Rise Direction
Without cell walls (Open Cell)

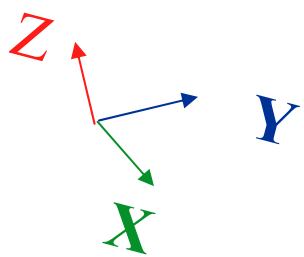

Max. Principal, 443MPa

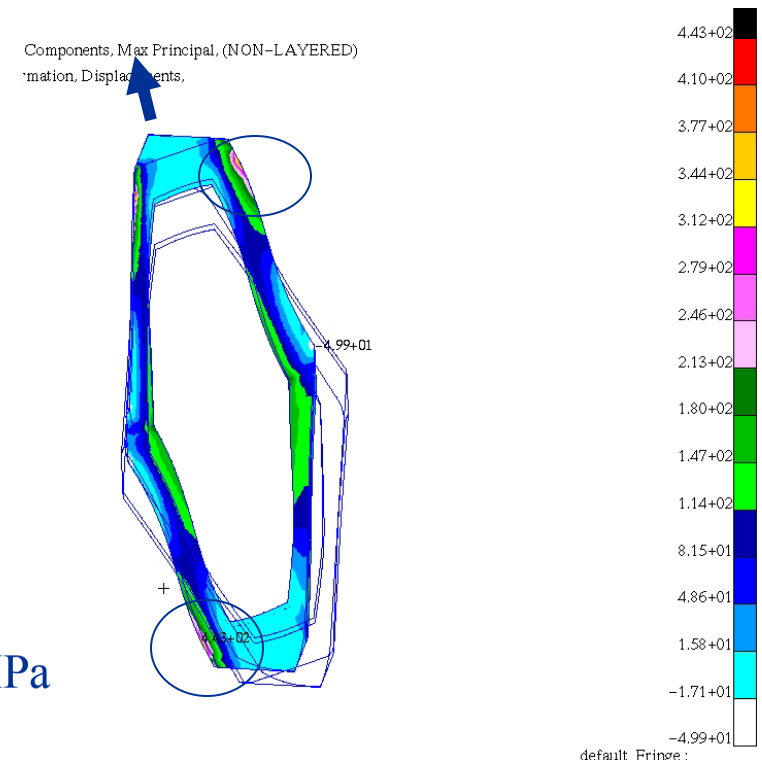

Open Cell Structure For Failure Analysis

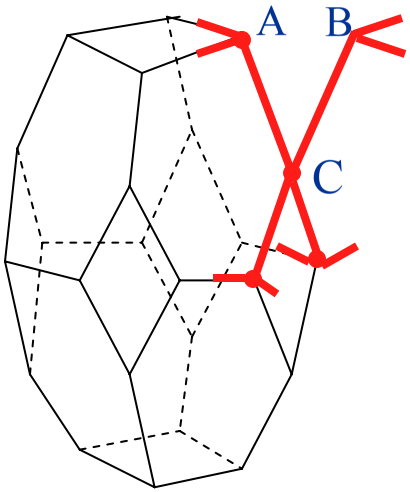

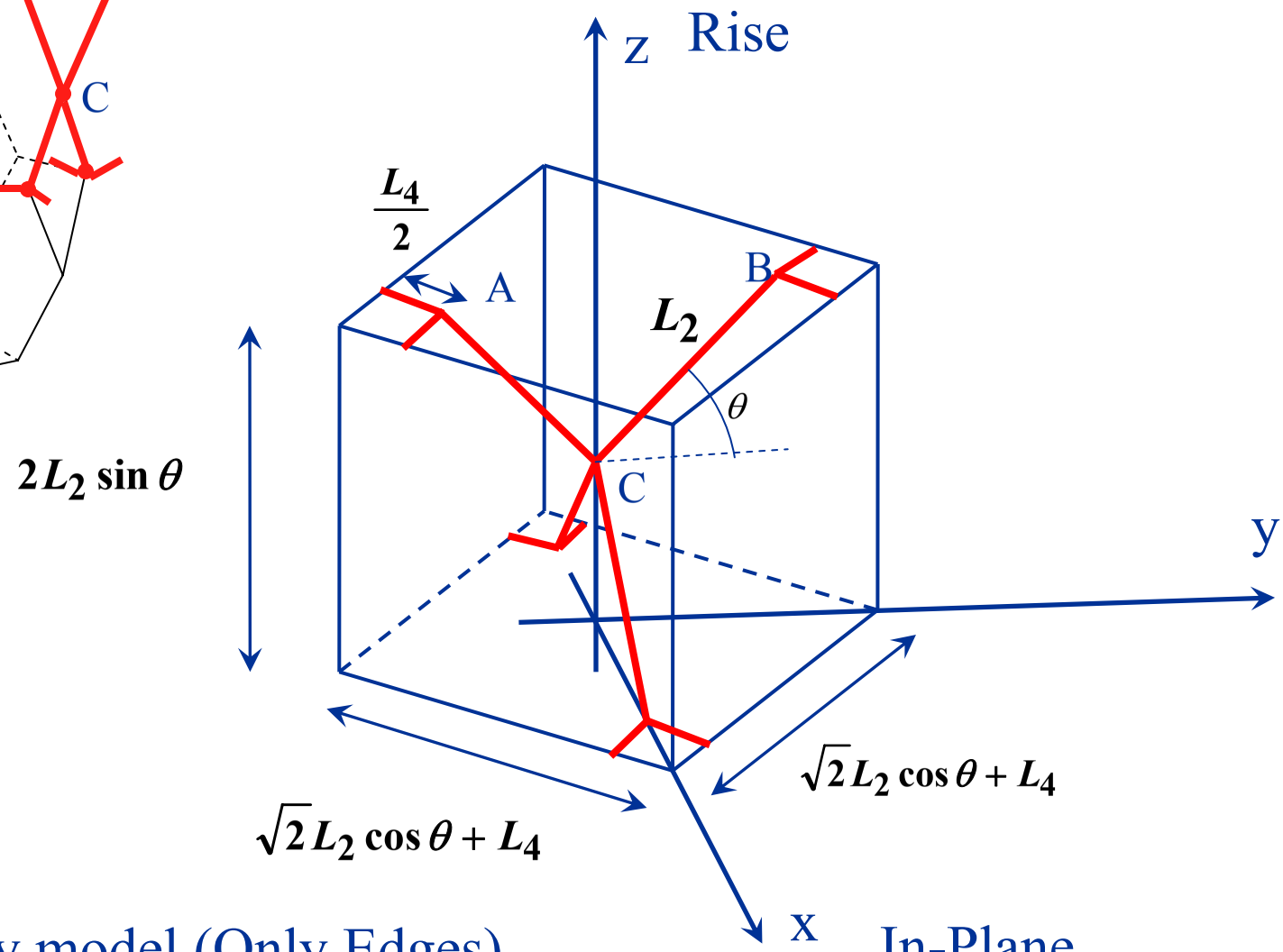

Simplify model (Only Edges)

In-Plane

Equilibrium and Structural Analysis of Frames yields

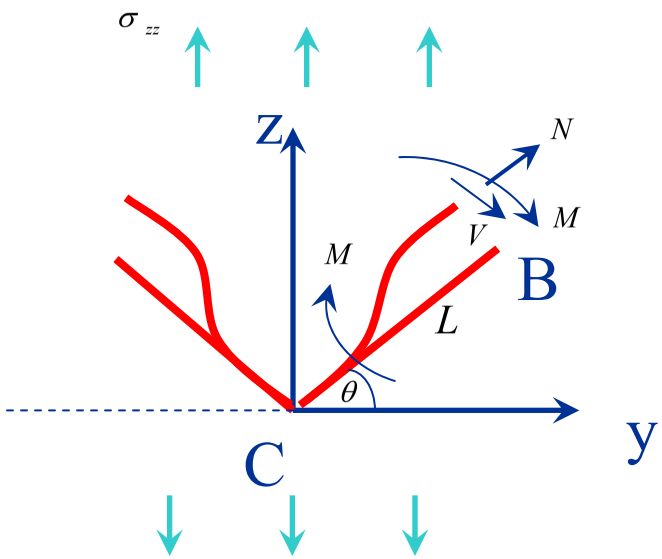

$$N = \frac{\sigma_{zz} \sin\theta \left[\sqrt{2}\, L_2 \cos\theta + L_4\right]^2}{2}$$

$$M = \frac{\sigma_{zz} L_2 \cos\theta \left[\sqrt{2}\, L_2 \cos\theta + L_4\right]^2}{4}$$

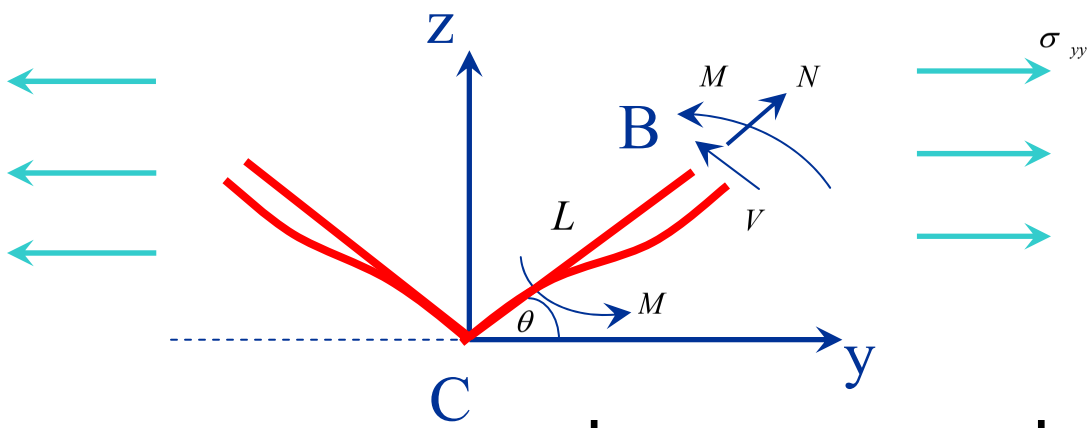

$$N = \sigma_{yy} L_2 \cos\theta \sin\theta \left[2 L_2 \cos\theta + \sqrt{2}\, L_4\right]$$

$$M = \frac{\sigma_{yy} L_2^2 \sin^2\theta \left[2 L_2 \cos\theta + \sqrt{2}\, L_4\right]}{2}$$

Strength of Materials approach for calculating the maximum stress at the outer fiber of an axial and flexural of the edges

$$\sigma_{\max} = \frac{N}{A} + \frac{Mr}{I}$$

Where
A = edge x-area
I = edge moment of Inertia
r = distance to outer fiber

Leads to the relation between the maximum stress in the struts and the average applied stress in the z and y directions:

$$\sigma_{zz} = \frac{\sigma_{\max}}{\left[\frac{\sin\theta}{2A} + \frac{L_2 r\cos\theta}{4I}\right]\left(\sqrt{2}L_2\cos\theta + L_4\right)^2}$$

$$\sigma_{yy} = \frac{\sigma_{\max}}{\left[\frac{L_2\cos\theta\sin\theta}{A} + \frac{L_2^2 r\sin^2\theta}{2I}\right]\left(2L_2\cos\theta + \sqrt{2}L_4\right)}$$

Calculating the average cell strain and stress can also lead to determining the effective cell modulus in two directions :

$$E_z = \frac{24 \quad EI\sin\theta}{L_2^2\left[\cos^2\theta + \frac{12I\sin^2\theta}{AL_2^2}\right]\left(\sqrt{2}L_2\cos\theta + L_4\right)^2}$$

$$E_y = \frac{12 \quad EI}{\left[2L_2^3\sin^2\theta + L_4^3 + \frac{12I}{A}\left(2L_2\cos^2\theta + L_4\right)\right]L_2\sin\theta}$$

Ratio of the Stiffness in the z- and y-directions is

$$\frac{E_z}{E_y} = \frac{2\sin^2\theta\left[2L_2^3\sin^2\theta + L_4^3 + \frac{12I}{A}\left(2L_2\cos^2\theta + L_4\right)\right]}{L_2\left[\cos^2\theta + \frac{12I\sin^2\theta}{AL_2^2}\right]\left[\sqrt{2}L_2\cos\theta + L_4\right]^2}$$

Assuming L_2 and L_4 are 69 μm and 28 μm, respectively, we can plot the stiffness ratio versus inclination angle.

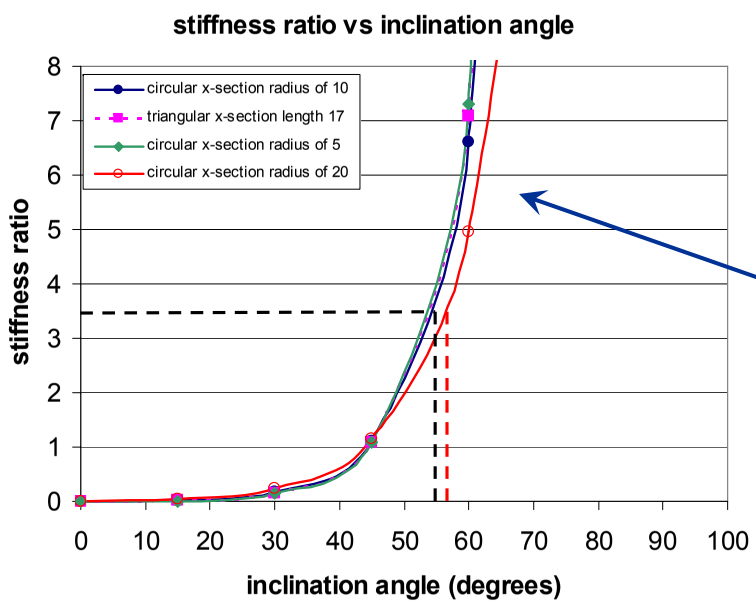

Measured stiffness ratio for BX-265 at room temperature

$$\frac{E_z}{E_y} = \frac{18MPa}{5MPa} = 3.6$$

Strut cross-section has small influence on stiffness ratio versus inclination angle

Results indicate that the inclination angle for BX-265 is ~55°

Ratio of strengths in z- and y-directions is

$$\frac{\sigma_z}{\sigma_y} = \frac{4L_2 \sin\theta\left[2I\cos\theta + L_2 rA\sin\theta\right]}{\left[2I\sin\theta + L_2 rA\cos\theta\right]\left[2L_2\cos\theta + \sqrt{2}L_4\right]}$$

From experimental tensile test specimen the measured ratio of the rise to in-plane strengths is approximately 1.6.

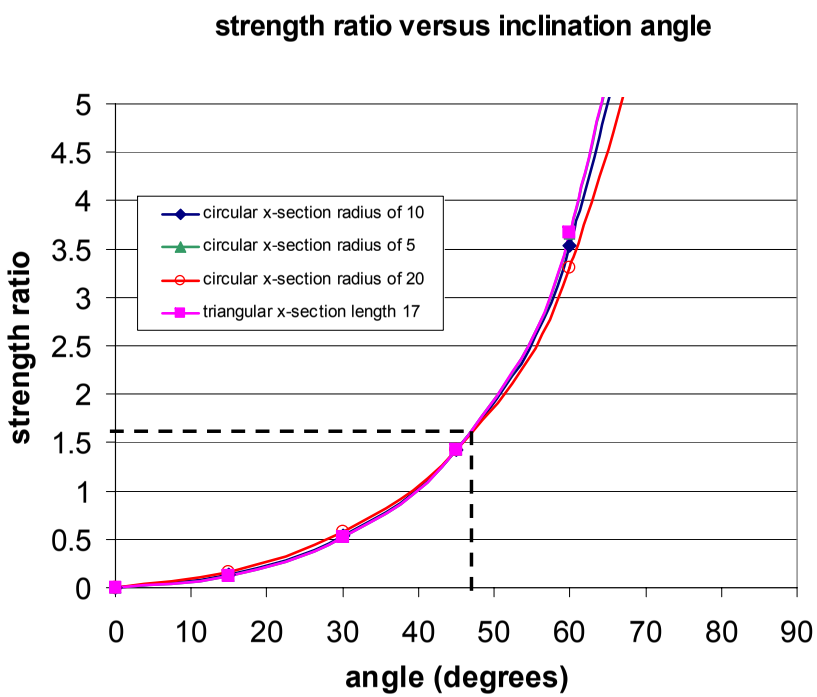

Results indicate that the inclination angle is 47°

Substituting L_2, L_4, and the inclination angle into the previous equations for foam modulus and foam strengths and solving for the polymer (strut) modulus and polymer (strut) strengths, we get

		Polymer (Strut) Modulus, MPa (ksi) Using $\theta = 55^o$	Polymer (Strut) Strength, MPa (ksi) Using $\theta = 47^o$
Circular x-section	R=5 μm	21,500 (3,120)	603 (87.5)
	R=10 μm	1,450 (210)	76 (11)
	R=20 μm	111 (16)	10 (1.5)
Triangular x-section 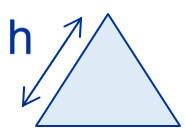 	h=17 μm	7,300 (1,059)	393 (57)

Summary

- SOFI microstructure were successfully modeled as elongated Tetrakaidechahedron closed cell
- Elastic modulus and Poisson's ratios were estimated from the unit cell model
- The estimation of the polymer solid strength and stiffness was attempted by FEA and Frame models.
- Frame model yields similar results as the finite element model if a circular cross-section with a radius of 10 mm is used.

Future Work

- Refine the FEA model (Nonlinearity) to improve on the failure stress estimates
- Review the modeling of a unit cell in vacuum